Spontaneous generation of prion infectivity in fatal familial insomnia knock-in mice

Citation: Jackson W.S., Borkowski A.W., Faas H., Steele A.D., King O.D., Watson N., Jasanoff A., Lindquist S. Spontaneous Generation of Prion Infectivity in Fatal Familial Insomnia Knockin Mice (2009) Neuron, 63 (4), pp. 438-450.

As Published: http://dx.doi.org/10.1016/j.neuron.2009.07.026

Publisher: Elsevier Inc.

Persistent URL: http://hdl.handle.net/1721.1/49488

Version: Author's final manuscript: final author's manuscript post peer review, without publisher's formatting or copy editing

Title: Spontaneous generation of prion infectivity in fatal familial insomnia knock-in mice

Authors: Walker S. Jackson, Andrew W. Borkowski, Henryk Faas, Oliver D. King, Andrew D. Steele, Nicki E. Watson, Alan Jasanoff, Susan Lindquist

Scientific grounds for submission to Neuron:
Prion diseases are transmissible fatal neurodegenerative diseases affecting humans and animals. The agents believed to cause these diseases are prions, infectious misfolded forms of the host-encoded PrP protein. Although supporting evidence exists, the crucial prediction that familial mutations can cause PrP to misfold into an infectious conformation has not been demonstrated. To test this prediction we generated mice to model fatal familial insomnia. They develop a disease which is very similar to the human form, and which is directly transmissible to mice expressing wild-type PrP. We provide the first unequivocal evidence that a protein carrying a familial mutation is sufficient to spontaneously generate infectious prion particles, providing long-sought critical support for the protein-only hypothesis. The countervailing theory that familial mutations simply sensitize carriers to exogenous sources appears incorrect.

Summary of paper's appeal to a popular audience:
In our early training as scientists, we are taught that the only bio-molecules responsible for storing information are nucleic acids. However the protein-only hypothesis states proteins can also store and transmit information. Moreover this information leads to very specific neurodegenerative diseases. We genetically modified mice to express the equivalent mutation causing fatal familial insomnia. These mice developed a disease with many of the features that distinguish human FFI from all other neurodegenerative diseases and, most importantly, this disease was transmissible to otherwise normal mice. Thus, our report bridges the fields of genetic and infectious diseases, and will also be of interest to the more general fields of sleep and neurodegenerative diseases.

Address for correspondence:
Susan Lindquist
Whitehead Institute for Biomedical Research
Nine Cambridge Center
Cambridge, MA 02142
Tel: 1- 617-258-5184 Fax: 1-617-258-7226
Email: lindquist_admin@wi.mit.edu

None of this work has been published or is under consideration elsewhere. Thank you for your consideration.

Spontaneous generation of prion infectivity in fatal familial insomnia knock-in mice

[1]Walker S. Jackson, [1,2]Andrew Borkowski, [3]Henryk Faas, [1]Andrew Steele, [1]Oliver D. King, [1]Nicki Watson, [3,4]Alan Jasanoff, [1,2]Susan Lindquist

[1] Whitehead Institute for Biomedical Research
Nine Cambridge Center
Cambridge, MA 02142

[2] Howard Hughes Medical Institute, Massachusetts Institute of Technology, Cambridge, MA 02142

[3] Frances Bitter Magnet Laboratory,
[4] Departments of Biological Engineering,
Brain & Cognitive Sciences, and
Nuclear Science & Engineering
Massachusetts Institute of Technology
150 Albany St., NW14–2213
Cambridge, MA 02139

Address correspondence to SL
Whitehead Institute for Biomedical Research
Nine Cambridge Center
Cambridge, MA 02142
lindquist_admin@wi.mit.edu
phone: 617-258-5184

SUMMARY

A crucial tenet of the prion hypothesis is that misfolding of the prion protein (PrP) induced by mutations associated with familial prion disease is, in an otherwise normal mammalian brain, sufficient to generate the infectious agent. Yet this has never been demonstrated. We engineered knock-in mice to express a PrP mutation associated with a distinct human prion disease, fatal familial insomnia (FFI). An additional substitution created a strong transmission barrier against pre-existing prions. The mice spontaneously developed a disease distinct from that of other mouse prion models and highly reminiscent of FFI. Unique pathology was transmitted from FFI mice to mice expressing wild-type PrP sharing the same transmission barrier. FFI mice were highly resistant to infection by pre-existing prions, confirming infectivity did not arise from contaminating agents. Thus a single amino acid change in PrP is sufficient to induce a distinct neurodegenerative disease and the spontaneous generation of prion infectivity.

De Novo Prions in Fatal Familial Insomnia Mice

INTRODUCTION

Prion diseases are a heterogeneous group of devastating and fatal neurodegenerative diseases affecting animals (chronic wasting disease in deer and elk, scrapie in goats and sheep, and “mad cow” disease in cattle) and humans (Creutzfeldt-Jakob disease, CJD; Gerstmann-Sträussler-Scheinker syndrome, GSS; fatal familial insomnia, FFI; and kuru

(Aguzzi et al., 2007; Prusiner, 1998). Sponge-like vacuolation, neuronal loss, and PrP deposits are commonly present but clinical symptoms and the types and distribution of neural lesions vary between different prion diseases (Prusiner, 1998). Prion diseases are highly unusual in that they can be acquired by infection, can occur sporadically, or can be inherited (Prusiner, 1998).

The agents most widely believed to cause these diseases are known as prions (Prusiner, 1982). Prions were originally defined as proteinaceous infectious particles, and later found to consist primarily of the misfolded host-encoded PrP protein (Prusiner, 1982, 1998). The protein-only hypothesis of infectivity is supported by many lines of evidence (Castilla et al., 2005; Collinge and Clarke, 2007; Deleault et al., 2007; Legname et al., 2004), yet an important element remains controversial (Chesebro, 2003; Manuelidis, 2007; Somerville, 2002; Weissmann and Flechsig, 2003). The hypothesis holds that a misfolded, self-templating form of PrP is the basis of infectivity. Further, PrP mutations that are associated with familial human prion disease produce infectivity by increasing the likelihood of the misfolding event. However, the crucial prediction that a disease-associated PrP mutation can, in fact, spontaneously generate infectivity has never been experimentally demonstrated. Of the many transgenic mouse models that have been studied, only one – expressing a PrP mutation associated with GSS – has been suggested to produce spontaneous infectivity (Hsiao et al., 1994; Hsiao et al., 1990). However, subsequent work established that brain homogenates of these mice are more properly described as "accelerating a pre-existing disease" in the GSS recipient mice (Nazor et al., 2005). Disease could not be transmitted to mice expressing wild-type PrP. Therefore, the countervailing theory, that PrP mutations simply make animals more

susceptible to infection by an exogenous agent, remains viable (Barron et al., 2001; Chesebro, 2003; Manson et al., 1999; Manuelidis, 2007; Weissmann and Flechsig, 2003).

To create a unique model of inherited prion disease and determine if familial PrP mutations can spontaneously give rise to infectivity, we engineered mice to express a PrP gene carrying the mouse equivalent of the human FFI mutation. This mutation was chosen because biophysical studies predict that its propensity to destabilize PrP is in the middle range of disease-associated PrP mutations (Apetri et al., 2004; Riek et al., 1998) and, more importantly, it is associated with FFI, a disease with a clinical spectrum and neuropathology distinct from other prion diseases (Gambetti and Lugaresi, 1998; Lugaresi et al., 1998). Distinguishing clinical features of FFI are disruption of the autonomic nervous system (dysautonomia) and a form of insomnia in which deep, slow wave sleep is not achieved (Benarroch and Stotz-Potter, 1998; Gambetti and Lugaresi, 1998; Lugaresi et al., 1986). (Secondary clinical manifestations include loss of muscle coordination (ataxia) and seizure-like muscle twitching, but these are also seen in other prion diseases.) Unlike other prion diseases, and indeed virtually any other neurodegenerative disease, the most striking neuropathology of FFI occurs in the thalamus, consisting of neuronal loss and reactive gliosis (Benarroch and Stotz-Potter, 1998; Gambetti and Lugaresi, 1998; Lugaresi et al., 1986; Lugaresi et al., 1998). Furthermore, most prion diseases demonstrate abundant proteinase K (PK)-resistant forms of PrP (PrP^{res}) and widespread spongiform degeneration, but FFI does not (Brown et al., 1995; Little et al., 1986; Lugaresi et al., 1986; Parchi et al., 1998). Indeed, classification of FFI as a prion disease was disputed (Little et al., 1986; Lugaresi et al., 1986) until it was linked to an aspartate- to- asparagine substitution at codon 178

(D178N) of the PrP gene (*Prnp*) (Medori et al., 1992) and shown to be transmissible (Collinge et al., 1995; Tateishi et al., 1995).

No mouse model fully recapitulates any human disease. But we hoped that the pathology associated with the FFI mutation would be both sufficiently reminiscent of the pathology of human FFI and, most importantly, sufficiently distinct from the pathology of other mouse prion models to ensure that disease was due to the FFI-mutated PrP protein. In the event that our mice developed a transmissible form of the disease, it was necessary to establish that the mutation didn't simply make the mouse more susceptible to contaminating pre-existing prions that might be present in our laboratory (Chesebro, 2003; Manuelidis, 2007; Somerville, 2002). Indeed, the familial mutation associated with GSS (P101L) makes mice more susceptible to prion infection (Barron et al., 2001; Manson et al., 1999). Hence, we altered two additional amino acids to introduce a transmission barrier (species barrier) to pre-existing prions (Scott et al., 1993; Supattapone et al., 2001), substituting two methionines from the wild-type human sequence for leucine and valine (at aa position 108 and 111) in the wild-type mouse sequence. Humanizing the prion sequence in this manner provided two additional important benefits. First it allowed us to distinguish the origin of any infectious material in transmission studies because the substitution allows recognition by the 3F4 antibody. Second, in previous transgenic mouse experiments, unmodified human or mouse sequences were much less efficient in modeling infectious human prion diseases than human/mouse chimeras which included the 3F4 epitope (Telling et al., 1995). This may be because some human sequences facilitate the misfolding that is presumed to occur

with the familial PrP mutations, because of host-specific PrP::chaperone interactions, or both.

Finally, over-expression of PrP makes mice more prone to spontaneous disease (Castilla et al., 2004; Westaway et al., 1994) and makes them more susceptible to prion infection (Fischer et al., 1996; Sigurdson et al., 2006; Thackray et al., 2002). Therefore, we used a knock-in approach to introduce the FFI mutation to the *Prnp* locus. This ensured that the allelic variants would remain subject to all of the regulatory elements that normally control the complex expression pattern of PrP (McCormack et al., 2002).

Knock-in mice carrying the FFI mutation developed biochemical, physiological, behavioral, and neuropathological abnormalities that were surprisingly similar to FFI in humans and very different from those of scrapie-infected mice or transgenic mice expressing other mutant forms of PrP. Remarkably, this spontaneous disease could be transmitted, and serially passaged, to mice expressing physiological amounts of wild-type PrP with the same human epitope. The FFI mice were highly resistant to common laboratory strains of mouse scrapie and the few mice that did succumb exhibited the characteristics of mouse scrapie rather than FFI. These data exclude the possibility that the spontaneous FFI disease and its transmissibility arose from infection with pre-existing prions. Knock-in mice carrying the 3F4 epitope alone never succumbed to spontaneous disease. Thus, the single amino acid substitution associated with FFI in humans causes spontaneous prion disease in mice. The transmissibility of this genetically initiated disease to mice not carrying the FFI mutations provides crucial support for a causal link between PrP misfolding and the spontaneous generation of a transmissible agent.

RESULTS

Generation of FFI mice

We generated two strains of mice expressing PrP proteins that differ only by a single amino acid (D177N), the mouse equivalent of the mutation associated with human FFI (Figure 1A). Both proteins also carried the two amino acid human sequence substitution (L108M, V111M). In addition to introducing a transmission barrier against mouse scrapie (Scott et al., 1993; Supattapone et al., 2001), this substitution introduced an epitope for the 3F4 antibody, which does not detect mouse PrP (Kascsak et al., 1987). These genes were inserted into their normal genomic context by gene-replacement in mouse embryonic stem (ES) cells (Figure S1) (Moore et al., 1995; Selfridge et al., 1992). ES cells were tested for homologous recombination by PCR (data not shown) and Southern analysis (Figure 1B) and positive ES cells were used to generate knock-in mice, designated ki-3F4-WT and ki-3F4-FFI. PCR analysis of homozygous animals amplified the modified allele but not the unmodified, wild-type (WT) allele (Figure 1B). Western blotting of brain homogenates showed no 3F4 immunoreactivity in brains of WT or PrP knock-out (KO) mice, but did show immunoreactivity in ki-3F4-WT and ki-3F4-FFI mice (Figure 1C).

PrP modified only by the 3F4 epitope (PrP^{3F4WT}) was expressed at the same level as unmodified wild-type PrP (PrP^{WT}), as shown by their equal reactivity with 6H4 antibody (Figure 1C). It also produced identical banding patterns as PrP^{WT}, before and after treatments with enzymes diagnostic for trafficking though the endoplasmic reticulum (ER) and Golgi (Fig 1d). Both proteins were sensitive to PNGaseF, indicating

they had entered the ER and became glycosylated, and were resistant to endoglycosidaseH, indicating they had trafficked to the Golgi for further sugar modification. Therefore, our gene targeting approach and the introduction of the 3F4 epitope did not cause any unintended changes to PrP levels or trafficking.

PrP that carried both the 3F4 epitope and the D177N substitution (PrP^{3F4FFI}) was, like PrP^{WT} and PrP^{3F4WT}, sensitive to PNGaseF but not endoglycosidaseH, indicating it too enters the ER and is trafficked to the Golgi. However, PrP^{3F4FFI} was expressed at reduced levels, as predicted for a protein prone to misfolding (Apetri et al., 2004; Riek et al., 1998) (Figure 1C). Importantly, as seen in humans with FFI (Parchi et al., 1998), the faster migrating unglycosylated form of PrP was nearly absent (Figure 1C) indicating that the FFI mutant protein was trafficked and post-translationally modified in mice in the same distinct manner as it is in humans.

Neuropathology of ki-3F4-FFI mice

Homozygous ki-3F4-WT mice did not get sick and exhibited no neuropathology. Heterozygous ki-3F4-FFI mice also appeared normal although they were examined less thoroughly. This was expected as humans carry the FFI mutation for decades prior to disease onset. We therefore focused on homozygous mice to increase gene dosage, a standard practice for knock-in mice modeling neurodegenerative diseases that require many years to develop in humans (Lin et al., 2001), and since homozygous carriers of prion mutations develop disease faster than heterozygotes {Simon, 2000 #2083). Many of the homozygous ki-3F4-FFI mice lived as long as ki-3F4-WT mice, but all developed

profound neuropathology and behavioral abnormalities. To visualize the effects of the FFI mutation on overall brain structure *in vivo* we employed a manganese-enhanced magnetic resonance imaging technique (Aoki et al., 2004; Faas et al., 2009). In contrast with age matched WT and ki-3F4-WT controls, at 16 months many ki-3F4-FFI mice had a flattened or concave motor cortex and an atrophied cerebellum (Figures 2A and S2). The ventricles were also greatly enlarged (Figure 2A), consistent with atrophy of underlying neural nuclei. Degenerated cerebella (Almer et al., 1999; Bar et al., 2002; Manetto et al., 1992; Sasaki et al., 2005) and dilated ventricles (Bar et al., 2002; Sasaki et al., 2005) have also been reported in human FFI cases. Most importantly, abnormalities of the thalamus were prominent (Figure 2A). This region of the brain, in addition to other critical brain functions, is thought to be important for sleep regulation (Huguenard and McCormick, 2007). Thalamic damage is a hallmark of human FFI (Lugaresi et al., 1986).

Paraffin-embedded brain sections were stained with hematoxylin and eosin (H&E). Gross examination revealed enlarged ventricles (~20 months, Figure 2B) and vacuolization, which was restricted to the deep cerebellar white matter (~16 months, Figure S5). We also employed immunohistochemistry (IHC) for glial fibrillary acidic protein (GFAP) to detect reactive gliosis, a conventional marker of neurodegeneration. We found strong GFAP immunostaining in the deep white matter of the cerebellum (n=16 of 24, ~16 months), especially in areas with vacuolization (Figure 2C) and also found strong GFAP staining in the thalamus first detected at 12 months (n=24 of 24, Figure 2D). In contrast, ki-3F4-WT mice lacked this abnormal GFAP staining both in the cerebellum (n=12; $p<0.0005$; Fisher's exact) and thalamus (n=12; $p<0.0001$). Closer

examination of H&E stained sections revealed areas of severe neuronal loss in the thalamus (~18 months, Figure 2E). As a complementary approach, with low power magnification we detected severe loss of thalamic neurons by examining 30-μm thick sections stained with a Nissl specific dye (~18 months, Figure S6). Thus, ki-3F4-FFI mice developed a unique pattern of neurodegeneration that is distinct from all other neurodegenerative diseases in humans and scrapie-infected mice but reminiscent of human FFI {Little, 1986 #1167; Lugaresi, 1986 #1166; Gambetti, 1995 #434}.

In most prion diseases, PrP acquires biophysical properties that render it partially resistant to digestion by PK , a state commonly called PrP^{res} (Prusiner, 1998). FFI, however, characteristically produces very little PrP^{res} and is often not detected (Brown et al., 1995; Medori et al., 1992; Parchi et al., 1998; Zarranz et al., 2005). In brains of spontaneously sick ki-3F4-FFI mice standard immunohistochemical experiments (data not shown) and western blotting experiments also using standard conditions, failed to demonstrate PrP^{res} (Figure 2F). We also did not detect distinct PrP conformers using conformation dependent immunoassays, histoblots, phosphotungstate precipitations, semi-denaturing detergent-agarose gel electrophoresis, luminescent conjugated polymers, and several immunohistochemical methods (utilizing various conditions of PK digestions, denaturants and autoclaving or microwaving steps, data not shown). However, when 20 mg of total brain homogenates from 2 year old ki-3F4-FFI mice was PK digested and concentrated by tricholoracetic acid precipitation, a small amount of PrP^{res} was detected (Figure 2F). Therefore, the unusual biochemical characteristic of producing low amounts of PrP^{res} in human FFI is also recapitulated in this mouse model.

Clinical abnormalities of ki-3F4-FFI mice

Behavioral changes were detected using automated mouse behavioral analysis (AMBA), which employs 24- hour video recordings to classify activities of mice in solitary cages (Steele et al., 2007). Videos are collected at a rate of 30 frames per second for 24hrs (~2.6 x 10E6 frames per session) and a series of 6 frames is sufficient to classify individual behaviors. This system allows the detection of phenotypic changes prior to overt abnormalities by quantifying changes in a large number of spontaneous activities and allowing the assessment of undisturbed nocturnal behavior (the active period for the mouse). Employing this technology previously, we uncovered an unexpected phenotype in scrapie infected mice: during the night they travel incessantly, covering ten times more distance than control mice (Steele et al., 2007). Here, we compared WT, ki-3F4-WT, and ki-3F4-FFI mice throughout their lives, with several early time points to establish a baseline before disease onset. WT and ki-3F4-WT mice behaved similarly throughout their lifetimes, indicating that neither the mixed genetic background we employed nor the 3F4 epitope caused behavioral abnormalities (Figure S7)

Ki-3F4-FFI mice developed striking age-related changes in behavior. A few individual behaviors, plotted over the course of 24 hrs for mice at 16 months of age are presented in Figure 3A. A composite of all the data for the different groups of mice is presented in Figure 3B in a "phenotypic array" format. The data for each behavior in a 24 hr period is collapsed into one tile. Each tile represents the median difference between the two genotypes for that behavior, with cyan indicating behaviors that decreased and yellow indicating behaviors that increased in ki-3F4-FFI mice compared to ki-3F4-WT

mice; the brightness of the color corresponds to the magnitude of the difference between the two groups.

Behavioral abnormalities in ki-3F4-FFI mice were most prominent at night (Fig 3A), but stood in sharp contrast to those of scrapie-infected mice. Rather than traveling more than controls (Steele et al., 2007), ki-3F4-FFI mice spent less time traveling and covered less distance (Figure 3A). They also spent less time jumping, hanging from the top of the cage, and rearing on their hind limbs (fully reared) than control mice, indicating a reduction in overall activity (Figures 3A and 3B), again opposite to scrapie infected mice (Steele et al., 2007). Strikingly, Ki-3F4-FFI mice had higher scores of awaken (activity that ends rest periods) and twitch (activity that disrupts rest periods), metrics of sleep interruption, starting as early as 5 months of age (Figure 3B). This occurred far before overt physical or behavioral abnormalities were apparent without AMBA (which occurred only at 12 to 16 months). Twitching during rest continued to increase and by 16 months ki-3F4-FFI mice exhibited extended periods of inactivity, lying on the cage floor (specifically in the night phase) as if they were exhausted from lack of uninterrupted sleep ("rest", Figures 3B and 3C).

Sleep state is tightly coupled with core body temperature (T_b), which rises during wake periods and declines during sleep (Mochizuki et al., 2006). Human FFI typically includes dysautonomia with abnormal T_b regulation (Lugaresi et al., 1986; Sasaki et al., 2005). To measure T_b we implanted small temperature-recording devices (Mochizuki et al., 2006) into the peritoneal cavity of five mice of each genotype at 16 months, and measured T_b at 5-minute intervals for ten days.

T_b fluctuated over a much wider range in ki-3F4-FFI mice than in ki-3F4-WT mice, routinely reaching below 35°C for 4 of the ki-3F4-FFI mice (Figures 3C and S8). The fifth mouse was instead persistently hyperthermic, (Figure 3C). The interrupted sleep measured by AMBA and the improperly controlled T_b suggests ki-3F4-FFI mice do not enter deep sleep. Humans with FFI typically appear hypersomnic because they enter the early stages of sleep yet are unable to enter deep, slow wave sleep (Lugaresi et al., 1986; Lugaresi et al., 1998). Thus, ki-3F4-FFI mice developed both activity and temperature homeostasis abnormalities reminiscent of human FFI.

Ki-3F4-FFI disease is transmissible

To test for the presence of a transmissible agent, we injected a relatively conservative amount of brain homogenate (30 µl dose of material diluted 1 to 100 m/v), intracranially. We employed recipient mice that expressed no PrP (KO) (Bueler et al., 1992; Manson et al., 1994), normal levels of PrP (WT or ki-3F4-WT), or high levels of PrP (Tga20) (Fischer et al., 1996).

The 3F4 epitope itself has been repeatedly tested and never found to produce infectious material on its own (Scott et al., 1993; Supattapone et al., 2001). However, to control for the possibility that the 3F4 epitope caused mouse PrP to spontaneously misfold in the knock-in configuration employed here, we aged ki-3F4-WT mice for two years to maximize the opportunity for spontaneous conversion. All genotypes injected with brain homogenate from these mice remained healthy until they were sacrificed in old age (Figures 4A and 4G-J).

To determine whether mice carrying the FFI mutation on the 3F4 background produced infectivity, we sacrificed 3 spontaneously sick (terminal) mice that had become symptomatic at different ages. Both Tga20 mice and ki-3F4-WT mice developed neurodegenerative disease.

Tga20 mice over-express PrP^{WT} from a randomly integrated transgene. Although over-expression of PrP can itself lead to pathology (Castilla et al., 2004; Westaway et al., 1994), Tga20 mice have been extensively characterized, with no spontaneous pathologies reported (Fischer et al., 1996; Sigurdson et al., 2009; Thackray et al., 2002). Because the over expression of PrP accelerates the course of disease (Fischer et al., 1996; Thackray et al., 2002), Tga20 mice are commonly used to test for the presence of infectious agents. Moreover, Tga20 mice are sensitive to prions with heterologous sequences (Sigurdson et al., 2006; Sigurdson et al., 2009). When injected with brain homogenates from spontaneously sick ki-3F4-FFI mice they developed ataxia, kyphosis (hunched back posture), pruritus (persistent itch), dermatitis, reduced body condition and a highly unusual paroxysmal hind limb tremor (Figure 4B and Movie S1). Neuropathological examination of injected Tga20 mice revealed intense GFAP immunoreactivity in the thalamus and enlargement of ventricles (Figures 4G and 4H). Importantly, homogenates made from all three of the spontaneously sick ki-3F4-FFI mice we tested produced similar physical symptoms, behavior, pathology and time course ($p>0.1$, log-rank; statistical tests for FFI transmission studies can be found in Supplemental table 1). Tga20 mice either not injected or injected with normal brain homogenates never displayed any of these abnormalities of behavior (Figure 4A, Movie S2) or histology (Figure 4H, right).

Thus, spontaneously sick ki-3F4-FFI mice generated a transmissible agent that produced a disease in Tga20 mice that has many unique features and is distinct from scrapie.

Even more tellingly, ki-3F4-WT mice, expressing normal levels of PrP, also became sick, developing ataxia, kyphosis, reduced body condition, and many died prematurely following injection with homogenates from spontaneously sick ki-3F4-FFI mice (Figure 4C). Of course, we would not expect the same pathology in mice suffering the effects of the continuous production of mutant, misfolding PrP throughout the brain throughout their lifetimes (primary FFI disease), as in mice expressing wild-type protein suffering the effects of a transmissible agent delivered in a single dose in one location. Indeed, the latter did not exhibit thalamic damage. They did, however, share other features of degenerative damage with spontaneously sick ki-3F4-FFI mice, including the absence of PrP^{res} (data not shown), dilated ventricles, white matter vacuolization and increased GFAP staining in the cerebellum (Figures 4I and 4J). The apparently different rates of disease onset, though not statistically significant ($p>0.5$), might reflect different prion titers in the primary inoculum or the presence of multiple prion strains (Polymenidou et al., 2005). The spontaneously generated disease of ki-3F4-FFI mice was caused by the FFI mutation and was transmissible to mice expressing endogenous levels of PrP.

We then asked if the infectivity observed with ki-3F4-FFI brain homogenates could be serially transmitted. Brain homogenates of sick ki-3F4-WT mice that had been injected with brain homogenates from spontaneously sick ki-3F4-FFI were injected into a fresh group of ki-3F4-WT mice. These second-passage recipient mice developed ataxia, kyphosis, reduced body condition, and died prematurely (Figure 4D). On histological

examination they had atrophy of subcortical regions and swelling of ventricles, similar to that of spontaneously sick ki-3F4-FFI mice and yet different from scrapie infected mice (Figure 4K). Not unexpectedly, the precise pathology that developed in mice injected with brain homogenates from spontaneously sick ki-3F4-FFI mice depended on the amount and/or sequence of PrP protein that was being expressed in the recipient animal (i.e. Tga20 or ki-3F4-WT). But the transmissible nature of the pathology was unequivocal.

As expected, PrP KO mice injected with brain homogenates from spontaneously sick ki-3F4-FFI mice remained normal behaviorally (Figure 4E) and neuropathologically (data not shown). Thus, as reported for all other transmissible prion agents, susceptibility to the agent produced by our FFI mice required that the animals be expressing PrP protein. Notably, however, wild-type mice injected with these homogenates also remained healthy (Figure 4F). The fact that transmission to hosts expressing physiological amounts of PrP required the 3F4 epitope indicates the transmissible agent produced by the FFI mice was sensitive to transmission barriers, much like typical prions (Aguzzi et al., 2007; Collinge and Clarke, 2007; Somerville, 2002). Since wild-type mice could not be infected, neither the ki-3F4-FFI mice nor the inocula derived from their brains were contaminated by preexisting agents.

Ki-3F4-FFI mice resist exogenous prions

The fact that brain homogenates of ki-3F4-FFI mice produced a disease with properties very different from that caused by mouse scrapie indicates that they are producing a unique new strain of prion infectivity. Is the spontaneous misfolding of the FFI mutant

PrP responsible for generating this transmissible agent? Or could the FFI mutation simply have made carriers more sensitive to an exogenous agent? (Barron et al., 2001; Chesebro, 2003; Manson et al., 1999; Manuelidis, 2007; Somerville, 2002; Weissmann and Flechsig, 2003). We employed the 3F4 epitope from human and hamster PrP in our experiments because it was reported to produce a transmission barrier, at least in a randomly integrated transgenic mouse model (Supattapone et al., 2001). To directly test whether FFI mice were more susceptible to pre-existing prions, we injected ki-3F4-WT mice with two different strains of mouse-adapted scrapie, RML and 22L, the only prion strains that have ever been employed on our campus. The 3F4 epitope created a very strong transmission barrier against both strains. Even when injected with ~10^7 infectious units of 22L or RML, ki-3F4-WT mice had longer incubation periods than did WT mice lacking the 3F4 epitope injected with only ~50 infectious units (Figure 5A) (statistical tests for scrapie transmission studies can be found in Table S2). To determine if the 3F4 transmission barrier applied to alternative routes of infection 22L scrapie was also injected intraperitoneally. Again, the 3F4 epitope introduced an extremely strong transmission barrier (Figure 5B). Therefore, ki-3F4-WT mice were resistant to contamination from conventional prions but were sensitive to *de novo* FFI prions.

Strikingly, mice carrying both the 3F4 epitope and the FFI mutation had an even stronger transmission barrier against RML and 22L mouse scrapie (Figure 5C), perhaps because of primary or tertiary structural differences between the inoculum and substrate or simply because there was a reduced steady state level of PrP in the brain of FFI mice (Figure 1C). Indeed, in only the most aggressive of six experiments (10^7 infectious units of 22L intracranially) did the injection of exogenous mouse prions shorten the lifespan of

ki-3F4-FFI mice (Figure 5D). When the mice injected with these high levels of prions became sick, they exhibited behaviors and pathology characteristic of scrapie-infected mice and very different from spontaneously sick 3F4-FFI mice. Moreover, as with scrapie, they produced easily detectable PrP^{res} with the typical cleavage of the N-terminus (Figure 5E). Since the 3F4 antibody will react with mouse PrP if carrying the 3F4 epitope but not with unmodified mouse PrP, this PrP^{res} material must have been synthesized by the host and was not simply residual material from the scrapie inoculum since it reacted with the 3F4 antibody (Figure 5E). Therefore, PrP^{3F4FFI} is competent to form PrP^{res} when templated by infection with laboratory prion strains. The dearth of PrP^{res} in our spontaneously sick ki-3F4-FFI mice, and in the animals that succumbed to the transmissible agent they produced, confirm that they had not been infected with scrapie.

Finally, although hamsters have never been housed in our facility nor have we ever passaged hamster scrapie in mice, we obtained hamster scrapie from the Rocky Mountain Laboratory and injected mice intracranially. Ki-3F4-FFI mice died at the same advanced age as ki-3F4-WT or WT mice (Figure 5F). Therefore, ki-3F4-FFI mice are not more sensitive to infection by exogenous prions.

DISCUSSION

Our work fulfills a long standing and long unfulfilled prediction of the prion hypothesis: in the context of an otherwise normal animal a familial mutation in PrP is sufficient to cause the *de novo* appearance of a transmissible agent for neurodegeneration. Mice

carrying the FFI mutation in PrP developed a spontaneous disease that was remarkably reminiscent of human FFI. Due to the fact that our mice produced infectious material, we were not permitted to perform polysomnography in any of the facilities we contacted. However, the overt sleep disturbances – rest and twitch during rest – we observed in video recordings and the extreme fluctuations in temperature provide strong evidence of sleep perturbations and dysautonomia. The biochemical properties of the PrP protein in our model, and the region-specific neuropathological abnormalities we observed were also akin to those of FFI.

Importantly, the phenotypic spectrum as a whole was distinct from those reported for any other PrP mouse models. Furthermore, the mice spontaneously generated prions which encoded "information" that led to distinct neuropathology when injected into tester animals, a pathology that was partially over lapping with spontaneous disease and, again, distinct from that of other previously described transmissible prion strains. Thus, the FFI mutation was sufficient to specify not only a unique disease state, but a unique self-perpetuating transmissible agent.

PrP^{res} is often considered a hallmark of prion disease and of the presence of a transmissible agent. However, in many cases of FFI (Brown et al., 1995; Little et al., 1986; Medori et al., 1992; Zarranz et al., 2005), as well as in certain other types of prion diseases (Barron et al., 2007; Haviv et al., 2008; Lasmezas et al., 1997; Manson et al., 1999), PrP^{res} is not detected. In fact, in a systematic survey of various forms of genetic and sporadic human prion diseases PrP^{res} was readily detectable in several disease types, but it was not detected in four out of four FFI samples using a relatively large sample of tissue, 0.2 gm (Brown et al., 1995). Indeed, it was only detectable when a full gram of

tissue – equivalent to 2.5 whole adult mouse brains – was employed (Brown et al., 1995). Moreover, transgenic mice expressing human PrP and injected with human FFI brain homogenates also failed to produce PrP^{res} despite developing a severe neuropathology (Collinge et al., 1995). The same mice injected with human CJD homogenates produced readily detectable PrP^{res} (Collinge et al., 1995). Thus negative results with the FFI samples were not just a peculiarity of that transgenic line. In separate experiments, PrP^{res} was abundant in the brains of humans who carried the FFI mutation but, notably, in these cases the wild-type allele carried the valine polymorphism at codon 129 or the FFI mutant allele itself carried an octapeptide deletion, (Parchi et al., 1995; Reder et al., 1995; Tateishi et al., 1995; Telling et al., 1996). Since our mice lacked these sequence differences, we predicted they would not generate high levels of PrP^{res} if they accurately modeled the human disease. This prediction was fulfilled. Whether the small amount of PrP^{res} we detect after concentrating brain homogenates constitutes the infectious agent in our mice, or some other as yet uncharacterized species, remains to be determined.

One suggestion from our work is that other mutations in PrP, which are associated with distinct disease pathologies in humans, might be expected to give rise to their own transmissible agents. However, several lines of mice expressing PrP with various familial mutations have been reported and none have been found to produce a transmissible agent. In fact, this failure has been widely cited as evidence against the prion hypothesis (Chesebro, 2003; Manuelidis, 2007; Somerville, 2002). Given our positive result, why might these other experiments have failed? One possibility is that most of these models employ randomly integrated transgenes, in which a mutant PrP allele, often carrying only a small fragment of the large and complex PrP promoter,

integrates into a random position of the genome, with a variable number of copies. This approach has been employed because it is far less labor intensive than the production of knock-in mice. Further, the integration of multiple copies (a characteristic of the method) allows for unusually high levels of PrP expression, which would quite reasonably be expected to increase the likelihood of conformational conversion. But the variable expression patterns obtained with these transgenes have contributed to highly variable phenotypes which often don't mimic human disease. Some lines are disease-free despite overall high PrP expression levels (DeArmond et al., 1997; Nazor et al., 2005), while other lines develop CNS disease but apparently no infectivity (Chiesa et al., 1998; Hegde et al., 1999). The spontaneous production of *de novo* prions was previously reported in just one case, for a randomly integrated transgene with the P101L mutation (Hsiao et al., 1994). However, the recipient animals for the inoculum over-expressed this same mutation at a lower level (Hsiao et al., 1994). In repetitions of this experiment such animals spontaneously developed disease without inoculation (Nazor et al., 2005) and disease could not be transmitted to mice not carrying the mutation (Hsiao et al., 1994; Nazor et al., 2005). This result was therefore reinterpreted to indicate that the inoculum merely accelerated the course of disease in mutant animals {Collinge, 2007 #2003; Nazor, 2005 #1972}.

Our ki-3F4-FFI mice were developed by replacing the endogenous PrP coding sequence with a PrP protein carrying the D177N mutation in the coding sequence, but leaving all of the native gene regulatory elements unchanged. It may be that PrP needs to be expressed in particular cell types at particular levels in order to generate the transmissible agent spontaneously. Indeed, changes in regulation driven by *Prnp's*

endogenous regulatory sequences in response to pathology may also play a role. In any case, the fact that such an agent was generated with endogenous levels of expression fulfills the prion hypothesis rigorously.

An approach like ours was, however, used to model GSS with the P101L mutation. Those mice did not get sick and did not generate a transmissible agent (Manson et al., 1999). One explanation for the difference in our results is that, in contrast with D177N, P101L is not located in the structured core of PrP (Riek et al., 1998). Thus it might not be subject to the same type of misfolding as our D177N mutation. Notably, both GSS and FFI typically appear in humans in mid life. However, once pathology occurs, GSS progresses much more slowly than FFI (average time to mortality 5 years after onset versus 1 year) (Kovacs et al., 2002). In mice, given their short life span, it might progress too slowly to manifest a detectable disease or to generate infectious material.

Another possible explanation is the 3F4 epitope which might enhance the effect of the D177N mutation on the misfolding of PrP. If so, then it is important that we included it, as it is present in the human sequence, the natural context of the FFI mutation. Importantly, the presence of this two amino acid substitution does not itself influence the stability of PrP (as judged by its steady-state accumulation and modification). And it does not cause disease nor produce infectivity, even when mice are aged for two full years to maximize the possibility of their producing infectious agents if they were so prone. Thus, even if the 3F4 epitope facilitates the production of a transmissible agent, the process is clearly driven by the FFI mutation.

Surprisingly, transgenic mice expressing high levels of fully human PrP carrying familial mutations were recently reported to be disease free (Asante et al., 2009). It may be that knock-in mice will be required, with PrP regulated by its endogenous gene regulatory elements. Alternatively, it might be necessary to employ chimeric mouse-human PrP proteins to sufficiently model inherited human prion diseases. Indeed previous experiments employing mice to test for the presence of a transmissible agent in brain samples from humans with familial disease established that chimeric proteins were much more effective than either fully human or fully mouse proteins (Telling et al., 1996; Telling et al., 1995). A particularly interesting explanation is that mouse-specific interaction sites for PrP co-factors or chaperones are required. Knock-in mouse experiments testing the FFI mutation in the context of fully mouse or fully human PrP will begin to address this interesting issue but, alas, will require an additional five to six years for completion.

Interestingly, a new randomly integrated transgenic mouse model was recently reported to have sleep abnormalities (Dossena et al., 2008; Fioriti et al., 2005). This transgene carried the D177N mutation and the 3F4 epitope, but it also carried the CJD-specific M128V polymorphism. However, in contrast with our study, transmissible prions were not reported. Moreover, the neuronal loss and spongiform degeneration characteristic of CJD (Gambetti et al., 1995) were not reported (Dossena et al., 2008). It would be interesting to compare our FFI knock-in mice with the randomly integrated FFI transgenics produced by the same group (Fioriti et al., 2005). But neither spontaneous disease nor the spontaneous generation of a transmissible agent has yet been reported for them.

Prion infectivity experiments with knock-in mice by their very nature take a long time. These experiments were initiated 6 years ago (18 months to target embryonic stem cells and derive stable colonies, 18 months for knock-in mice to develop full blown age-dependent neurodegeneration, 3 years for serial transmission). Recently, another paper reported the spontaneous appearance of infectivity from a variant PrP sequence (Sigurdson et al., 2009). This contemporaneous study used very different methods and sequences. It did not involve a familial mutation as did ours, did not employ a species transmission barrier, and could only transmit to mice over-expressing PrP (Tga20). Importantly, however, it employed a cervid variant that is of great interest from a public health standpoint (chronic wasting disease of deer and elk) (Sigurdson et al., 2009). Together our work and theirs establish unequivocally that small sequence changes in PrP are sufficient to create a transmissible conformation.

The primary reason to model human neurodegenerative disease in mice is to generate a mammalian brain that undergoes a similar neurodegenerative process as in humans, but this is rarely accomplished. In addition to providing important new insight for prion biology, our mice develop biochemical, physiological, behavioral, and neuropathological abnormalities reminiscent of the human disease. These mice will be an invaluable resource in studies to uncover the mechanism of action of FFI and for test trials of potential treatments for this dreaded disease.

EXPERIMENTAL PROCEDURES

Mutagenesis of ES cells

Our double replacement gene-targeting strategy (Selfridge et al., 1992) was similar to one described previously for the *Prnp* gene (Moore et al., 1995) but with a few changes (Supplement methods and Figure S1).

Western Blotting

Brains were homogenized using safe-grind® tissue grinders (Wheaton, Millville, NJ), in standard buffer (PBS supplemented with 150 mM NaCl, 1% TritonX100, 4mM EDTA, and mini protease inhibitor cocktail tablets (Roche, Indianapolis, IN). For PNGaseF and EndoH experiments, 10% homogenates (100mg/ml tissue; 10mg/ml protein) were made in a hypotonic lysis buffer (10 mM Tris pH 7.5; 10 mM NaCl; 3 mM $MgCl_2$; 0.05% NP40; plus Roche protease inhibitor tablets). Reactions were set up as suggested by the supplier (New England Biolabs) with PMSF added. Reactions were incubated for 3 hours although one hour was sufficient to appropriately remove the glycans from AMOG, our internal control. Reactions were stopped by adding 50µl 4x Stop buffer. 20 µl (50 µg of total protein) were used per lane for electrophoresis. Several attempts to perform reactions overnight resulted in reduction of total PrP signal, indicating long incubations at 37°C results in degradation of PrP despite the addition of multiple protease inhibitors. For PK experiments, 10% brain homogenates made in PBS, then diluted into 2X conversion buffer, resulting in 300 mM NaCl, 1% TritonX100, 4mM EDTA, and 0.1M phosphate buffer. Total brain protein was incubated at a concentration of 5 mg/ml was incubated at 37°C for 30 minutes with 25 µg/ml enzyme grade PK.

Anti-PrP antibodies SAF32 (1:1,000; Cayman Chemical, Ann Arbor, MI), SAF61 (1:1,000; Cayman Chemical, Ann Arbor, MI), SAF 83 (1:2,000; Cayman Chemical, Ann

Arbor, MI), 3F4 (1:1K), 6H4 (1:5,000; Prionics, Schlieren, Switzerland), 7D9 (1:2,000; Abcam, Cambridge, MA). If scrapie infected samples were probed then antibodies were diluted an additional 5 fold. Other primary antibodies used: AMOG (adhesion molecule on glia or Na+, K+ ATPase subunit beta 2; 1:10K) and anti-actin (1:3,000; Sigma, St. Louis, Missouri). The actin primary antibody was a rabbit polyclonal and all others were mouse monoclonal. Blots in figure 1 were probed with secondary antibodies labeled with infrared fluorescent probes and scanned with the Odyssey imaging system (LI-COR Biosciences, Lincoln, Nebraska). Blots in figures 2 and 5 were probed with horseradish peroxidase labeled secondary antibodies and exposed to film.

Transmission experiments

Brains were homogenized with unused, safe-grind® tissue grinders, in 10 volumes of PBS. Experimental and control homogenates were sonicated (Misonix processor XL, Farmingdale, NY) using a cup horn set to power 9 for two 1 minute pulses. Prior to injection into recipient mice, homogenates were diluted to a specific concentration in PBS with 2% fetal bovine serum and sonicated for 1 minute at power 9. Homogenates were injected either intracranially (30 µl) or intraperitoneally (100 µl) using sterile 26 gauge needles into isoflurane anesthetized mice. A guide limiting the needle depth to 3.5 mm was used for intracranial injections. Inoculants from scrapie infected mice varied in concentration from 0.001% to 1%, as indicated on graphs, while all inoculants from spontaneously sick ki-3F4-FFI or ki-3F4-FFI infected mice were 1%, diluted in PBS only. Spontaneously sick ki-3F4-FFI mice were injected into tga20 mice homozygous for the transgene array for the first two experiments and hemizygous for the third primary

passage. Infected mice were inspected for general markers of poor health (kyphosis, ataxia, priapism, coarse coat, etc.) two to three times per week for scrapie experiments and 3 to 4 times per month for FFI transmission experiments. Graphs depict time to terminal illness for scrapie experiments and time until clear neurological disease in FFI experiments (two or more symptoms or a specific symptom on repeated health checks, since some were not terminally symptomatic prior to the end of the experiments. Neuropathology investigation verified neurodegenerative disease.

Neuropathology

Fixed brain tissues were embedded in paraffin prior to cutting into 4 μm sections, some of which were then stained with hematoxylin and eosin. We often preserved mouse brains by emersion fixation in formalin (Sigma), as this method allowed us to freeze one hemisphere as well. We also routinely transcardially perfusion fixed brains using formalin (Sigma), paraformaldehyde (Sigma), or Bouin's fixative (RICCA chemical co., Arlington, TX). The same neuropathological changes were detected regardless of the fixation method used. 30 micron sections of formalin fixed brains were also cut using a vibratome. Vibratome sections were subsequently stained with a fluorescent Nissl stain (Molecular Probes, Invitrogen).

IHC was performed on 4 micron paraffin embedded sections. Sections were dewaxed in zylenes and rehydrated in graded dilutions of ethanol. Epitope retrieval was performed with microwave irradiation in 0.01M citrate buffer. After removing endogenous peroxidase and blocking in 4 % normal horse serum, samples were incubated with

primary antibody in 2% serum/PBS overnight at 4°C in a wet incubation chamber. Samples were then incubated for 1 hr at room temperature with a biotinylated secondary antibody followed by incubation for 1 hr at room temperature with streptavidin-peroxidase (Vectastain Elite ABC kit (Universal, PK-6200)), with thorough PBS washing between incubation steps. A nickel enhanced diaminobenzidine substrate (Pierce, Rockford, Illinois) was used for detection. Primary antibodies; anti-PrP SAF32, 1:100, (Cayman Chemical, Ann Arbor, MI) anti-GFAP ascites MAB360, 1:10,000 dilution, Chemicon, Temecula, CA.

Magnetic resonance imaging

For magnetic resonance imaging we used a contrast enhancement (Lin and Koretsky, 1997) protocol we found capable of detecting subtle abnormalities in a different mouse model of neurodegenerative disease (Faas et al., 2009). Mice were injected intraperitoneally with 37.7 mg/kg $MnCl_2$, 1 day prior to imaging. For imaging, mice were anesthetized with isoflurane, and motion was suppressed using a stereotaxic frame. Mice were imaged on a Bruker 4.7 Tesla scanner using a surface coil and a T_1-weighted gradient echo pulse sequence (TE = 6 msec, TR = 50 msec, 6 averages) with a field of view of 2.0x2.0x1.0 cm and a matrix size of 160x160x80, for a total scan time of 64 minutes.

AMBA recordings

Following weaning, mice were designated for behavioral experiments and permanently housed in a suite of isolation cubicles dedicated to behavioral experiments. Mice were video recorded at 2, 3, 4, 5, 6, 8, 10, 12 16, 20, and 24 months of age. Mice were housed

in cages of up to four, and were separated from their cage mates into individual cages, immediately prior to video recording. The standard white lights automatically turn off after one hour of recording and turn on after 13 hours of recording. Dim red lights, which rodents do not see, illuminate the mice during the dark phase. After the 24 hour recording period, mice were placed into fresh cages with their original cage mates. To reduce the likelihood of fighting, especially upon re-introduction, only female mice were used in AMBA experiments. More details, including definitions of behaviors and validation tests of the software used are described in (Steele et al., 2007).

Temperature measurements

Core T_b was measured using iButtons model 1922L (Maxim, Dallas, TX) which have a resolution of 0.067°C. IButtons were implanted in the intraperitoneal cavity of anesthetized mice. The first week after surgery was considered a recovery phase and data from this period were not considered.

Acknowledgements

We thank M. Topolszki, A. Topolski, and J. Liu for technical assistance, D. Melton for mouse ES cells and related PrP plasmids, A. Aguzzi, M. Glatzel, M. Zabel, and C. Sigurdson for teaching us methods for mouse scrapie experiments, R. Bronson for neuropathology consultation, T. Scammell for advice on temperature recordings, and for critical review of the manuscript by C. Pacheco, J. Kritzer, J. Su, K. Matlack, D. Tardiff and especially K. Allendoerfer. This work was supported by funding from the Department of Defense (SL and AJ) and an NIH postdoctoral fellowship (WSJ).

FIGURE LEGENDS

Figure 1. Modification of PrP gene and protein by gene-targeting

(A) Schematic of modifications made to the Prnp locus, not to scale. Horizontal black line represents double stranded DNA, large grey box represents exon 3 containing all modifications, including the mutation of interest and a new BamHI site ("B") and small inserts for PCR genotyping (small grey box topped by "i" and flanked by arrows).

(B) Analysis of genome manipulation. Top, Southern analysis of mouse ES cells using BamHI and a probe (P) that does not anneal to the targeting vector. WT, untargeted DNA, targeted, indicates ES clones with knock-in alleles and a new 5 kilobase band (*). Left, bars indicate 10, 8, 6, and 5kb. Bottom, PCR analysis of mouse tail tip DNA from wild-type (WT), heterozygous (het), and homozygous knock-in (hom) mice. The product derived from the knock-in allele is indicated by *. The reduced migration rate of the highest band in lane two is the result of an open loop in heteroduplex PCR products. Left, bars indicate 250 and 200 bp.

(C) Western blot of KO (PrP knock-out), WT, ki-3F4-WT, and ki-3F4-FFI whole brain samples, probed with 3F4 PrP Ab, which detects only PrP that has been engineered to include the 3F4 epitope (top), probed with 6H4 antibody which detects all mouse PrP (middle), or with an actin antibody as a loading control (lower). Unglycosylated PrP is apparently absent in ki-3F4-FFI brains (top two blots, *).

(D) Biochemical analysis of posttranslational modification of PrP. Western blot of untreated and endoglycosidase H (endoH) and PNGaseF (lanes 9-12) treated samples, probed with SAF32 anti-PrP (top) from KO, WT, ki-3F4-WT (3F4/WT), and ki-3F4-FFI

(3F4/FFI) mice. Left, bars indicate 37 and 25 kDa. The same blot was stripped and probed with an antibody specific for adhesion molecule on glia protein (AMOG), a protein sensitive to both enzymes (lower). This control indicates equal loading and activity of EndoH and PNGaseF. Left, bars indicate 50, 37, and 25 kDa.

Figure 2. Neuropathology of ki-3F4-FFI mice

(A) MRI scans show enlarged ventricles (vent), atrophied cerebella (cb, arrowheads), and reduced signal intensity in the thalamus (thal,*) of ki-3F4-FFI mice (right) but not ki-3F4-WT mice (left).

(B) Low magnification of H&E stained brain sections shows enlarged ventricles in an FFI mouse (right, arrow and V) above the hippocampus (H) not present in ki-3F4-WT mice (left). Arrows in (A) bottom right and (B), right correspond to the same unusual gap or ventricle due to cortical atrophy.

(C) GFAP immunohistochemistry (GFAP) shows reactive gliosis (dark brown staining) and vacuolization (white rounded spots inside the GFAP stained area) in the cerebellar granular (g) and white matter (wm) in ki-3F4-FFI brains (right), but not ki-3F4-WT mice (left). The molecular (m) and Purkinge (P) cell layers are labeled for orientation.

(D) Reactive gliosis in the thalamus in ki-3F4-FFI mice (right), but not ki-3F4-WT mice (left).

(E) H&E shows loss of neurons (arrow, right) and increased numbers of glia (arrowheads, right) in the thalamus of ki-3F4-FFI mice compared to the thalamus of age matched ki-3F4-WT mice (left).

(F) Western analysis of brain homogenates (5 mg/ml protein) from aged WT, ki-3F4-WT (3F4/WT), or three sick ki-3F4-FFI mice (3F4/FFI), incubated for 1 hour with (+) or without (-) 25 mg/ml PK, and probed with 3F4 (left blot). PK digested samples were also concentrated prior to western blotting (right blot). Bars left of each blot indicate molecular weight in kDa. Faint bands with an apparent molecular weight of 25 kDa are likely not PrP since it was detected in WT mice with the 3F4 antibody. Each lane was loaded with 50 µg of total brain protein for the left blot; 2 mg of total protein for PK+ lanes and 50 µg for PK- lanes for the right blot.

Figure 3. Behavioral abnormalities in ki-3F4-FFI mice

(A) AMBA data of ki-3F4-FFI mice (blue lines) compared to ki-3F4-WT mice (red lines) at 16 months of age, show night time specific difference for distance traveled (top), fully reared (2^{nd} from top), twitch at rest (3^{rd} from top) and rest (bottom). Horizontal axes mark 24 one hour bins. The grey shading indicates the time at which lights are off (bins 2-13). P values are symbolized by * = $p< 0.05$, # = $p<0.01$, $ = $p<0.001$. Vertical error bars depict quartiles, and connecting lines intersect at the median.

(B) A phenotypic array representing median differences between ki-3F4-WT and ki-3F4-FFI mice for specific behaviors, labeled on the left. Yellow tiles depict comparisons for which the ki-3F4-FFI mice performed the specific activity more than ki-3F4-WT, and cyan tiles represent comparisons where the ki-3F4-FFI mice performed the specific activity less than ki-3F4-WT mice. The brightness corresponds to the magnitude of the difference (a scale is below the arrays). The age in months is labeled directly below the array. The number of animals for each comparison is immediately above the array where

"n_1" rows indicate the number of ki-3F4-WT mice and "n_2" rows indicate the number of ki-3F4-FFI mice.

(C) Body temperatures (T_b) were measured in 5 ki-3F4-WT and 5 ki-3F4-FFI mice at an accuracy of 0.067°C, using an implanted recorder. The T_b of a ki-3F4-WT (left WT individual 1, red) is plotted over the average T_b of 5 ki-3f4-WT mice (left, WT avg, black). Two ki-3F4-FFI mice (middle and left, FFI individual 1 and 2 respectively) are depicted by blue traces and are plotted over the same WT avg line. FFI mouse 1 had a widely fluctuating T_b while FFI mouse 2 had a persistently warm T_b.

Figure 4. Transmission of disease from ki-3F4-FFI brain homogenates

(A) Kaplan-Meier plot of Tga20 (square) and ki-3F4-WT (diamond) mice injected with 30 µl of 1% brain homogenate from 2 year old ki-3F4-WT mice. These mice never showed signs of disease.

(B-E) Kaplan-Meier plots of KO (B), WT (C), Tga20 (D), ki-3F4-WT (E), mice injected with 30 µl of 1% brain homogenates from 3 different spontaneously sick ki-3F4-FFI mice (FFI #1-3).

(F) Serial passage of ki-3F4-FFI disease from isolates (30 µl of 1% brain homogenates) derived from two separate ki-3F4-WT mice injected with FFI # 1 (E).

(G) Reactive gliosis detected by GFAP IHC was prominent in the thalamus of tga20 mice injected with brains of aged ki-3F4-FFI mice (dark staining, left) but not tga20 mice injected with brains from aged ki-3F4-WT mice (right).

(H) Enlarged ventricles (left, "V" and arrow) above the hippocampus ("H") were also prominent in tga20 mice injected with brain homogenates from aged ki-3F4-FFI mice,

but not in tga20 mice injected with brain homogenates from aged ki-3F4-WT mice (right).

(I) Reactive gliosis detected by GFAP IHC (darkly stained area) and vacuolization was prominent in the white matter of ki-3F4-WT mice injected with ki-3F4-FFI brain homogenate (left). A ki-3F4-WT mouse brain injected with brain homogenates from an aged ki-3F4-WT mouse has only background levels of GFAP staining and no vacuolization (right).

(J)Enlarged ventricle (left, arrow) above the hippocampus (Hipp) of a ki-3F4-wt mouse injected with brain homogenate from a sick ki-3F4-FFI mouse, not present in ki-3F4-WT mice injected with aged ki-3F4-WT brains (right).

(K) Enlarged ventricle above the hippocampus of a ki-3F4-WT mouse injected with brain homogenate from a sick ki-3F4-WT mouse previously injected with ki-3F4-FFI brain homogenate, not present in ki-3F4-WT mice succumbing to 22L scrapie prions (right).

Figure 5. FFI mice are not sensitized to common prion strains

(A-D) Kaplan-Meier survival plots showing the time to terminal illness following injection of 22L or RML strains of mouse adapted scrapie. Horizontal axes represent time in days from the date of injection except for panel d, where it represents the age of the mice (injected at ~ 40 days). (A) Ki-3F4-WT mice had longer incubation periods following intracranial injection with high titers (hi) of 22L ($10^{6.7}$ infectious doses (ID) or RML ($10^{6.5}$ ID, empty triangles) compared to similarly injected WT mice (filled and empty squares respectively) or WT mice injected with low titers (low) of 22L ($10^{1.7}$ ID, filled diamonds) or RML ($10^{1.5}$ ID, empty diamonds). (B) Ki-3F4-WT mice are resistant

to intraperitoneal injection of $10^{3.7}$ ID of 22L (filled triangles) compare to WT mice (filled squares). (C) Ki-3F4-FFI mice injected with either $10^{6.7}$ ID of 22L (filled circles) or $10^{3.5}$ ID of RML (empty circles) develop terminal illness later than similarly injected ki-3F4-WT mice (filled and empty triangles, respectively). (D) Ki-3F4-FFI mice injected with a high dose of 22L ($10^{6.7}$ ID, filled circles) develop a scrapie like disease and die earlier than uninjected mice (+) or mice injected with brain homogenate from an aged but otherwise normal mouse (*). (E) Brain homogenates (5 mg/ml) from WT, ki-3F4-WT (3F4/WT), or ki-3F4-FFI mice (3F4/FFI), terminally sick following injection with 22L mouse scrapie, were incubated for 1 hour with (+) or without (-) 25 mg/ml PK, and analyzed by western blotting. The 3F4 antibody detects a PrP^{res} species in ki-3F4-WT and ki-3F4-FFI mice, indicating it is not residual material from the inoculum. SAF32 detected undigested but not PK digested samples as the epitope in conventional PrP^{res} species is typically cleaved by PK.

(F) Kaplan-Meier survival plots showing mice expressing the 3F4 epitope are not sensitized to infection by hamster derived scrapie strain 263K.

Aguzzi, A., Heikenwalder, M., and Polymenidou, M. (2007). Insights into prion strains and neurotoxicity. Nat Rev Mol Cell Biol *8*, 552-561.

Almer, G., Hainfellner, J.A., Brucke, T., Jellinger, K., Kleinert, R., Bayer, G., Windl, O., Kretzschmar, H.A., Hill, A., Sidle, K.*, et al.* (1999). Fatal familial insomnia: a new Austrian family. Brain *122 (Pt 1)*, 5-16.

Aoki, I., Wu, Y.J., Silva, A.C., Lynch, R.M., and Koretsky, A.P. (2004). In vivo detection of neuroarchitecture in the rodent brain using manganese-enhanced MRI. Neuroimage *22*, 1046-1059.

Apetri, A.C., Surewicz, K., and Surewicz, W.K. (2004). The effect of disease-associated mutations on the folding pathway of human prion protein. J Biol Chem *279*, 18008-18014.

Asante, E.A., Gowland, I., Grimshaw, A., Linehan, J.M., Smidak, M., Houghton, R., Osiguwa, O., Tomlinson, A., Joiner, S., Brandner, S.*, et al.* (2009). Absence of

spontaneous disease and comparative prion susceptibility of transgenic mice expressing mutant human prion proteins. J Gen Virol *90*, 546-558.
Bar, K.J., Hager, F., Nenadic, I., Opfermann, T., Brodhun, M., Tauber, R.F., Patt, S., Schulz-Schaeffer, W., Gottschild, D., and Sauer, H. (2002). Serial positron emission tomographic findings in an atypical presentation of fatal familial insomnia. Arch Neurol *59*, 1815-1818.
Barron, R.M., Campbell, S.L., King, D., Bellon, A., Chapman, K.E., Williamson, R.A., and Manson, J.C. (2007). High titers of transmissible spongiform encephalopathy infectivity associated with extremely low levels of PrPSc in vivo. J Biol Chem *282*, 35878-35886.
Barron, R.M., Thomson, V., Jamieson, E., Melton, D.W., Ironside, J., Will, R., and Manson, J.C. (2001). Changing a single amino acid in the N-terminus of murine PrP alters TSE incubation time across three species barriers. Embo J *20*, 5070-5078.
Benarroch, E.E., and Stotz-Potter, E.H. (1998). Dysautonomia in fatal familial insomnia as an indicator of the potential role of the thalamus in autonomic control. Brain Pathol *8*, 527-530.
Brown, P., Kenney, K., Little, B., Ironside, J., Will, R., Cervenakova, L., Bjork, R.J., San Martin, R.A., Safar, J., Roos, R., and et al. (1995). Intracerebral distribution of infectious amyloid protein in spongiform encephalopathy. Ann Neurol *38*, 245-253.
Bueler, H., Fischer, M., Lang, Y., Bluethmann, H., Lipp, H.P., DeArmond, S.J., Prusiner, S.B., Aguet, M., and Weissmann, C. (1992). Normal development and behaviour of mice lacking the neuronal cell-surface PrP protein. Nature *356*, 577-582.
Castilla, J., Gutierrez-Adan, A., Brun, A., Doyle, D., Pintado, B., Ramirez, M.A., Salguero, F.J., Parra, B., Segundo, F.D., Sanchez-Vizcaino, J.M.*, et al.* (2004). Subclinical bovine spongiform encephalopathy infection in transgenic mice expressing porcine prion protein. J Neurosci *24*, 5063-5069.
Castilla, J., Saa, P., Hetz, C., and Soto, C. (2005). In vitro generation of infectious scrapie prions. Cell *121*, 195-206.
Chesebro, B. (2003). Introduction to the transmissible spongiform encephalopathies or prion diseases. Br Med Bull *66*, 1-20.
Chiesa, R., Piccardo, P., Ghetti, B., and Harris, D.A. (1998). Neurological illness in transgenic mice expressing a prion protein with an insertional mutation. Neuron *21*, 1339-1351.
Collinge, J., and Clarke, A.R. (2007). A general model of prion strains and their pathogenicity. Science *318*, 930-936.
Collinge, J., Palmer, M.S., Sidle, K.C., Gowland, I., Medori, R., Ironside, J., and Lantos, P. (1995). Transmission of fatal familial insomnia to laboratory animals. Lancet *346*, 569-570.
DeArmond, S.J., Sanchez, H., Yehiely, F., Qiu, Y., Ninchak-Casey, A., Daggett, V., Camerino, A.P., Cayetano, J., Rogers, M., Groth, D.*, et al.* (1997). Selective neuronal targeting in prion disease. Neuron *19*, 1337-1348.
Deleault, N.R., Harris, B.T., Rees, J.R., and Supattapone, S. (2007). Formation of native prions from minimal components in vitro. Proc Natl Acad Sci U S A *104*, 9741-9746.
Dossena, S., Imeri, L., Mangieri, M., Garofoli, A., Ferrari, L., Senatore, A., Restelli, E., Balducci, C., Fiordaliso, F., Salio, M.*, et al.* (2008). Mutant prion protein expression

causes motor and memory deficits and abnormal sleep patterns in a transgenic mouse model. Neuron *60*, 598-609.
Faas, H., Jackson, W.S., Borkowski, A., Wang, X., Ma, J., Lindquist, S., and Jasanoff, A. (2009). Context-dependent perturbation of neural systems
in transgenic mice expressing a neurotoxic prion protein. Submitted.
Fioriti, L., Dossena, S., Stewart, L.R., Stewart, R.S., Harris, D.A., Forloni, G., and Chiesa, R. (2005). Cytosolic prion protein (PrP) is not toxic in N2a cells and primary neurons expressing pathogenic PrP mutations. J Biol Chem *280*, 11320-11328.
Fischer, M., Rulicke, T., Raeber, A., Sailer, A., Moser, M., Oesch, B., Brandner, S., Aguzzi, A., and Weissmann, C. (1996). Prion protein (PrP) with amino-proximal deletions restoring susceptibility of PrP knockout mice to scrapie. Embo J *15*, 1255-1264.
Gambetti, P., and Lugaresi, E. (1998). Conclusions of the symposium. Brain Pathol *8*, 571-575.
Gambetti, P., Parchi, P., Petersen, R.B., Chen, S.G., and Lugaresi, E. (1995). Fatal familial insomnia and familial Creutzfeldt-Jakob disease: clinical, pathological and molecular features. Brain Pathol *5*, 43-51.
Haviv, Y., Avrahami, D., Ovadia, H., Ben-Hur, T., Gabizon, R., and Sharon, R. (2008). Induced neuroprotection independently from PrPSc accumulation in a mouse model for prion disease treated with simvastatin. Arch Neurol *65*, 762-775.
Hegde, R.S., Tremblay, P., Groth, D., DeArmond, S.J., Prusiner, S.B., and Lingappa, V.R. (1999). Transmissible and genetic prion diseases share a common pathway of neurodegeneration. Nature *402*, 822-826.
Hsiao, K.K., Groth, D., Scott, M., Yang, S.L., Serban, H., Rapp, D., Foster, D., Torchia, M., Dearmond, S.J., and Prusiner, S.B. (1994). Serial transmission in rodents of neurodegeneration from transgenic mice expressing mutant prion protein. Proc Natl Acad Sci U S A *91*, 9126-9130.
Hsiao, K.K., Scott, M., Foster, D., Groth, D.F., DeArmond, S.J., and Prusiner, S.B. (1990). Spontaneous neurodegeneration in transgenic mice with mutant prion protein. Science *250*, 1587-1590.
Huguenard, J.R., and McCormick, D.A. (2007). Thalamic synchrony and dynamic regulation of global forebrain oscillations. Trends Neurosci *30*, 350-356.
Kascsak, R.J., Rubenstein, R., Merz, P.A., Tonna-DeMasi, M., Fersko, R., Carp, R.I., Wisniewski, H.M., and Diringer, H. (1987). Mouse polyclonal and monoclonal antibody to scrapie-associated fibril proteins. J Virol *61*, 3688-3693.
Kovacs, G.G., Trabattoni, G., Hainfellner, J.A., Ironside, J.W., Knight, R.S., and Budka, H. (2002). Mutations of the prion protein gene phenotypic spectrum. J Neurol *249*, 1567-1582.
Lasmezas, C.I., Deslys, J.P., Robain, O., Jaegly, A., Beringue, V., Peyrin, J.M., Fournier, J.G., Hauw, J.J., Rossier, J., and Dormont, D. (1997). Transmission of the BSE agent to mice in the absence of detectable abnormal prion protein. Science *275*, 402-405.
Legname, G., Baskakov, I.V., Nguyen, H.O., Riesner, D., Cohen, F.E., DeArmond, S.J., and Prusiner, S.B. (2004). Synthetic mammalian prions. Science *305*, 673-676.
Lin, C.H., Tallaksen-Greene, S., Chien, W.M., Cearley, J.A., Jackson, W.S., Crouse, A.B., Ren, S., Li, X.J., Albin, R.L., and Detloff, P.J. (2001). Neurological abnormalities in a knock-in mouse model of Huntington's disease. Hum Mol Genet *10*, 137-144.

Lin, Y.J., and Koretsky, A.P. (1997). Manganese ion enhances T1-weighted MRI during brain activation: an approach to direct imaging of brain function. Magn Reson Med *38*, 378-388.
Little, B.W., Brown, P.W., Rodgers-Johnson, P., Perl, D.P., and Gajdusek, D.C. (1986). Familial myoclonic dementia masquerading as Creutzfeldt-Jakob disease. Ann Neurol *20*, 231-239.
Lugaresi, E., Medori, R., Montagna, P., Baruzzi, A., Cortelli, P., Lugaresi, A., Tinuper, P., Zucconi, M., and Gambetti, P. (1986). Fatal familial insomnia and dysautonomia with selective degeneration of thalamic nuclei. N Engl J Med *315*, 997-1003.
Lugaresi, E., Tobler, I., Gambetti, P., and Montagna, P. (1998). The pathophysiology of fatal familial insomnia. Brain Pathol *8*, 521-526.
Manetto, V., Medori, R., Cortelli, P., Montagna, P., Tinuper, P., Baruzzi, A., Rancurel, G., Hauw, J.J., Vanderhaeghen, J.J., Mailleux, P., and et al. (1992). Fatal familial insomnia: clinical and pathologic study of five new cases. Neurology *42*, 312-319.
Manson, J.C., Clarke, A.R., Hooper, M.L., Aitchison, L., McConnell, I., and Hope, J. (1994). 129/Ola mice carrying a null mutation in PrP that abolishes mRNA production are developmentally normal. Mol Neurobiol *8*, 121-127.
Manson, J.C., Jamieson, E., Baybutt, H., Tuzi, N.L., Barron, R., McConnell, I., Somerville, R., Ironside, J., Will, R., Sy, M.S.*, et al.* (1999). A single amino acid alteration (101L) introduced into murine PrP dramatically alters incubation time of transmissible spongiform encephalopathy. Embo J *18*, 6855-6864.
Manuelidis, L. (2007). A 25 nm virion is the likely cause of transmissible spongiform encephalopathies. J Cell Biochem *100*, 897-915.
McCormack, J.E., Baybutt, H.N., Everington, D., Will, R.G., Ironside, J.W., and Manson, J.C. (2002). PRNP contains both intronic and upstream regulatory regions that may influence susceptibility to Creutzfeldt-Jakob Disease. Gene *288*, 139-146.
Medori, R., Montagna, P., Tritschler, H.J., LeBlanc, A., Cortelli, P., Tinuper, P., Lugaresi, E., and Gambetti, P. (1992). Fatal familial insomnia: a second kindred with mutation of prion protein gene at codon 178. Neurology *42*, 669-670.
Mochizuki, T., Klerman, E.B., Sakurai, T., and Scammell, T.E. (2006). Elevated body temperature during sleep in orexin knockout mice. Am J Physiol Regul Integr Comp Physiol *291*, R533-540.
Moore, R.C., Redhead, N.J., Selfridge, J., Hope, J., Manson, J.C., and Melton, D.W. (1995). Double replacement gene targeting for the production of a series of mouse strains with different prion protein gene alterations. Biotechnology (N Y) *13*, 999-1004.
Nazor, K.E., Kuhn, F., Seward, T., Green, M., Zwald, D., Purro, M., Schmid, J., Biffiger, K., Power, A.M., Oesch, B.*, et al.* (2005). Immunodetection of disease-associated mutant PrP, which accelerates disease in GSS transgenic mice. Embo J *24*, 2472-2480.
Parchi, P., Castellani, R., Cortelli, P., Montagna, P., Chen, S.G., Petersen, R.B., Manetto, V., Vnencak-Jones, C.L., McLean, M.J., Sheller, J.R., and et al. (1995). Regional distribution of protease-resistant prion protein in fatal familial insomnia. Ann Neurol *38*, 21-29.
Parchi, P., Petersen, R.B., Chen, S.G., Autilio-Gambetti, L., Capellari, S., Monari, L., Cortelli, P., Montagna, P., Lugaresi, E., and Gambetti, P. (1998). Molecular pathology of fatal familial insomnia. Brain Pathol *8*, 539-548.

Polymenidou, M., Stoeck, K., Glatzel, M., Vey, M., Bellon, A., and Aguzzi, A. (2005). Coexistence of multiple PrPSc types in individuals with Creutzfeldt-Jakob disease. Lancet Neurol *4*, 805-814.
Prusiner, S.B. (1982). Novel proteinaceous infectious particles cause scrapie. Science *216*, 136-144.
Prusiner, S.B. (1998). Prions. Proc Natl Acad Sci U S A *95*, 13363-13383.
Reder, A.T., Mednick, A.S., Brown, P., Spire, J.P., Van Cauter, E., Wollmann, R.L., Cervenakova, L., Goldfarb, L.G., Garay, A., Ovsiew, F., and et al. (1995). Clinical and genetic studies of fatal familial insomnia. Neurology *45*, 1068-1075.
Riek, R., Wider, G., Billeter, M., Hornemann, S., Glockshuber, R., and Wuthrich, K. (1998). Prion protein NMR structure and familial human spongiform encephalopathies. Proc Natl Acad Sci U S A *95*, 11667-11672.
Sasaki, K., Doh-ura, K., Wakisaka, Y., Tomoda, H., and Iwaki, T. (2005). Fatal familial insomnia with an unusual prion protein deposition pattern: an autopsy report with an experimental transmission study. Neuropathol Appl Neurobiol *31*, 80-87.
Scott, M., Groth, D., Foster, D., Torchia, M., Yang, S.L., DeArmond, S.J., and Prusiner, S.B. (1993). Propagation of prions with artificial properties in transgenic mice expressing chimeric PrP genes. Cell *73*, 979-988.
Selfridge, J., Pow, A.M., McWhir, J., Magin, T.M., and Melton, D.W. (1992). Gene targeting using a mouse HPRT minigene/HPRT-deficient embryonic stem cell system: inactivation of the mouse ERCC-1 gene. Somat Cell Mol Genet *18*, 325-336.
Sigurdson, C.J., Manco, G., Schwarz, P., Liberski, P., Hoover, E.A., Hornemann, S., Polymenidou, M., Miller, M.W., Glatzel, M., and Aguzzi, A. (2006). Strain fidelity of chronic wasting disease upon murine adaptation. J Virol *80*, 12303-12311.
Sigurdson, C.J., Nilsson, K.P., Hornemann, S., Heikenwalder, M., Manco, G., Schwarz, P., Ott, D., Rulicke, T., Liberski, P.P., Julius, C.*, et al.* (2009). De novo generation of a transmissible spongiform encephalopathy by mouse transgenesis. Proc Natl Acad Sci U S A *106*, 304-309.
Somerville, R.A. (2002). TSE agent strains and PrP: reconciling structure and function. Trends Biochem Sci *27*, 606-612.
Steele, A.D., Jackson, W.S., King, O.D., and Lindquist, S. (2007). The power of automated high-resolution behavior analysis revealed by its application to mouse models of Huntington's and prion diseases. Proc Natl Acad Sci U S A *104*, 1983-1988.
Supattapone, S., Muramoto, T., Legname, G., Mehlhorn, I., Cohen, F.E., DeArmond, S.J., Prusiner, S.B., and Scott, M.R. (2001). Identification of two prion protein regions that modify scrapie incubation time. J Virol *75*, 1408-1413.
Tateishi, J., Brown, P., Kitamoto, T., Hoque, Z.M., Roos, R., Wollman, R., Cervenakova, L., and Gajdusek, D.C. (1995). First experimental transmission of fatal familial insomnia. Nature *376*, 434-435.
Telling, G.C., Parchi, P., DeArmond, S.J., Cortelli, P., Montagna, P., Gabizon, R., Mastrianni, J., Lugaresi, E., Gambetti, P., and Prusiner, S.B. (1996). Evidence for the conformation of the pathologic isoform of the prion protein enciphering and propagating prion diversity. Science *274*, 2079-2082.
Telling, G.C., Scott, M., Mastrianni, J., Gabizon, R., Torchia, M., Cohen, F.E., DeArmond, S.J., and Prusiner, S.B. (1995). Prion propagation in mice expressing human

and chimeric PrP transgenes implicates the interaction of cellular PrP with another protein. Cell *83*, 79-90.
Thackray, A.M., Klein, M.A., Aguzzi, A., and Bujdoso, R. (2002). Chronic subclinical prion disease induced by low-dose inoculum. J Virol *76*, 2510-2517.
Weissmann, C., and Flechsig, E. (2003). PrP knock-out and PrP transgenic mice in prion research. Br Med Bull *66*, 43-60.
Westaway, D., DeArmond, S.J., Cayetano-Canlas, J., Groth, D., Foster, D., Yang, S.L., Torchia, M., Carlson, G.A., and Prusiner, S.B. (1994). Degeneration of skeletal muscle, peripheral nerves, and the central nervous system in transgenic mice overexpressing wild-type prion proteins. Cell *76*, 117-129.
Zarranz, J.J., Digon, A., Atares, B., Rodriguez-Martinez, A.B., Arce, A., Carrera, N., Fernandez-Manchola, I., Fernandez-Martinez, M., Fernandez-Maiztegui, C., Forcadas, I., *et al.* (2005). Phenotypic variability in familial prion diseases due to the D178N mutation. J Neurol Neurosurg Psychiatry *76*, 1491-1496.

Figure 1

Jackson et al. 2009; Figure 1.

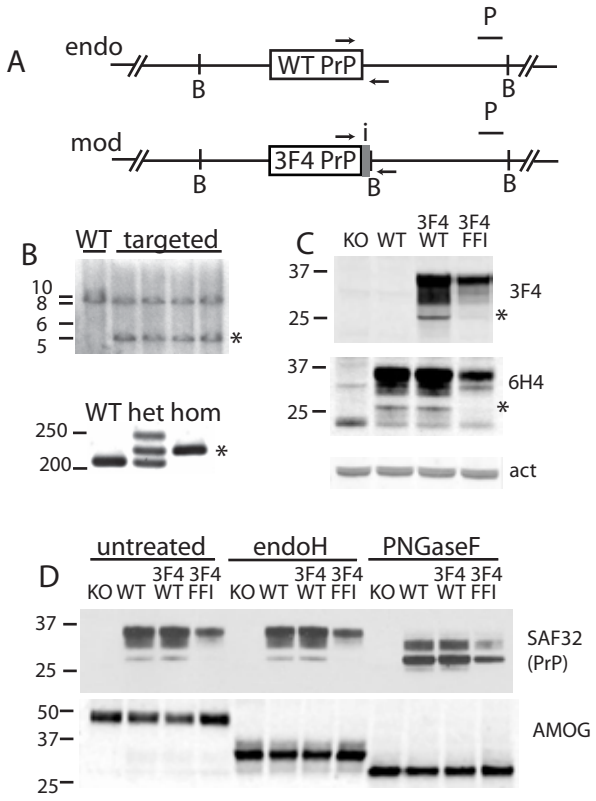

Figure 2

Jackson, 2009 Figure 2.

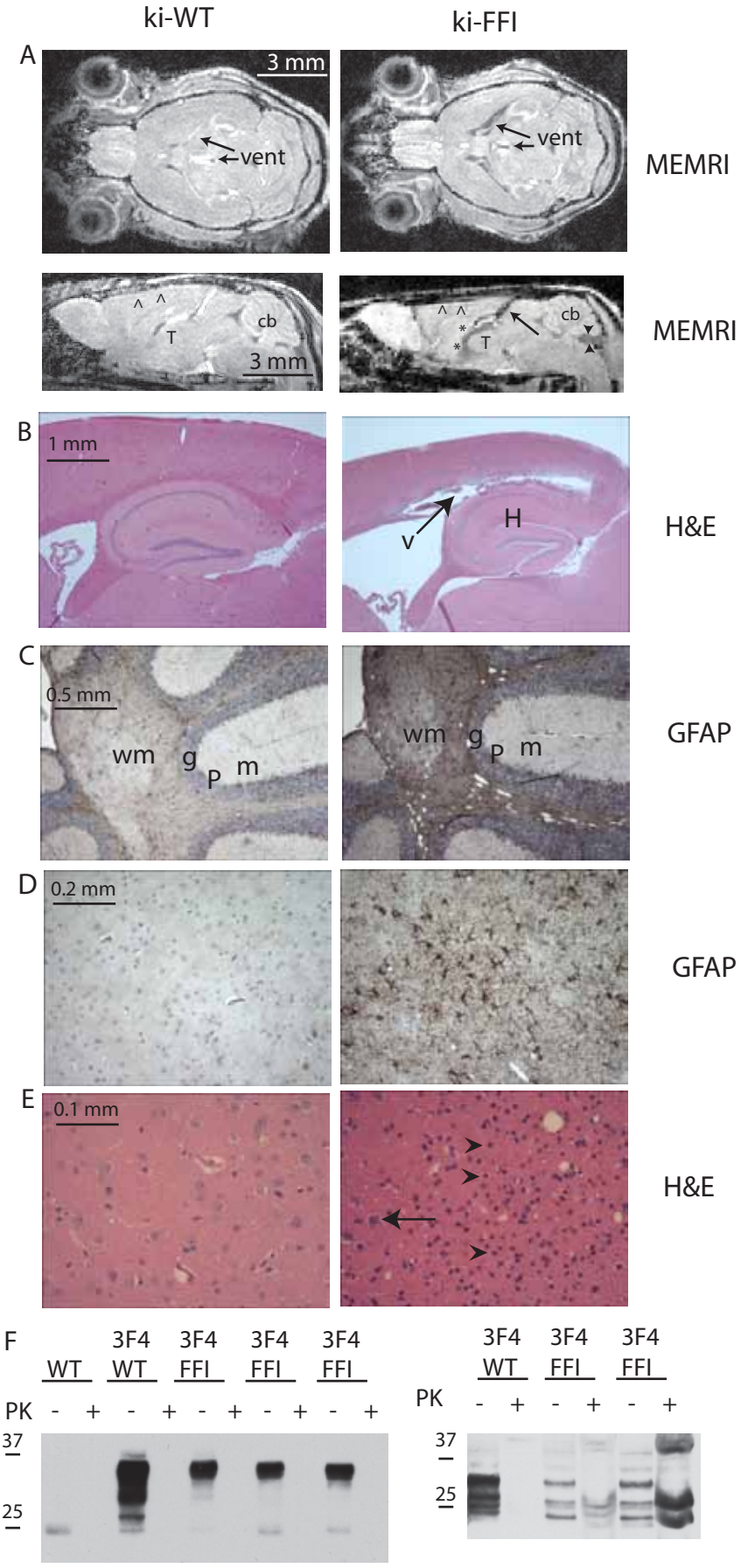

Figure 3

Jackson et al., Figure 3.

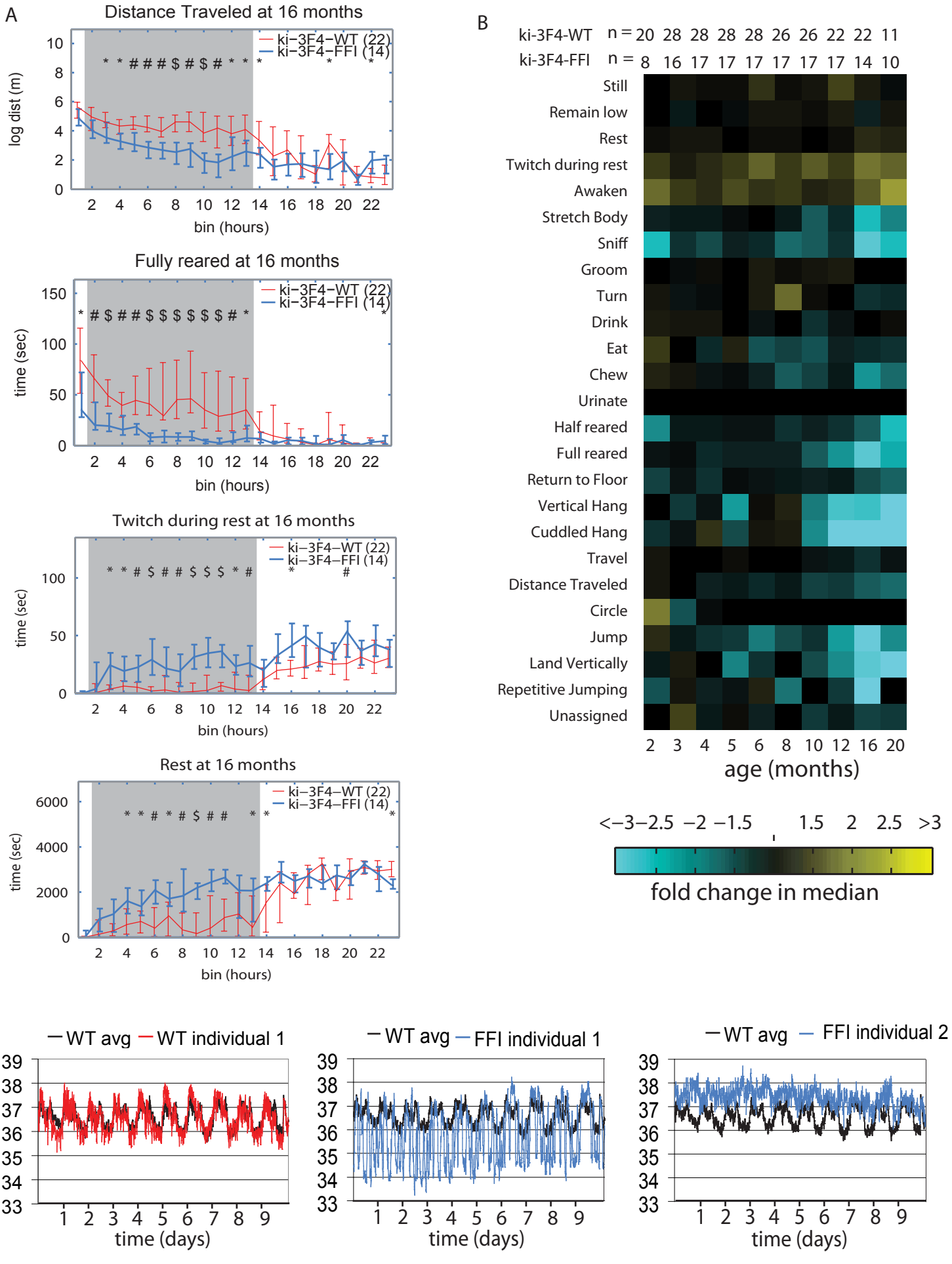

Figure 4

Jackson et al., Figure 4.

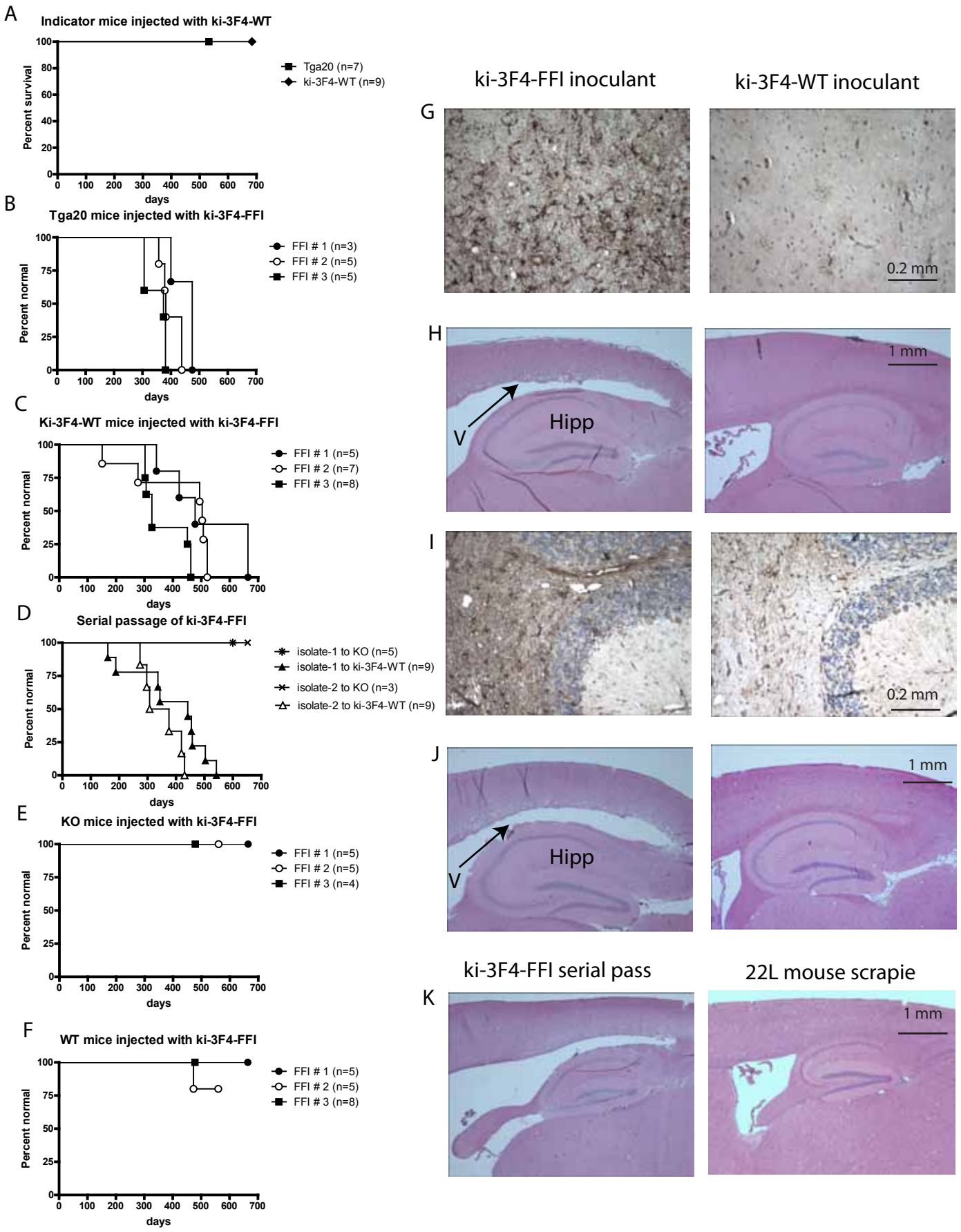

Figure 5

Jackson et al., Figure 5.

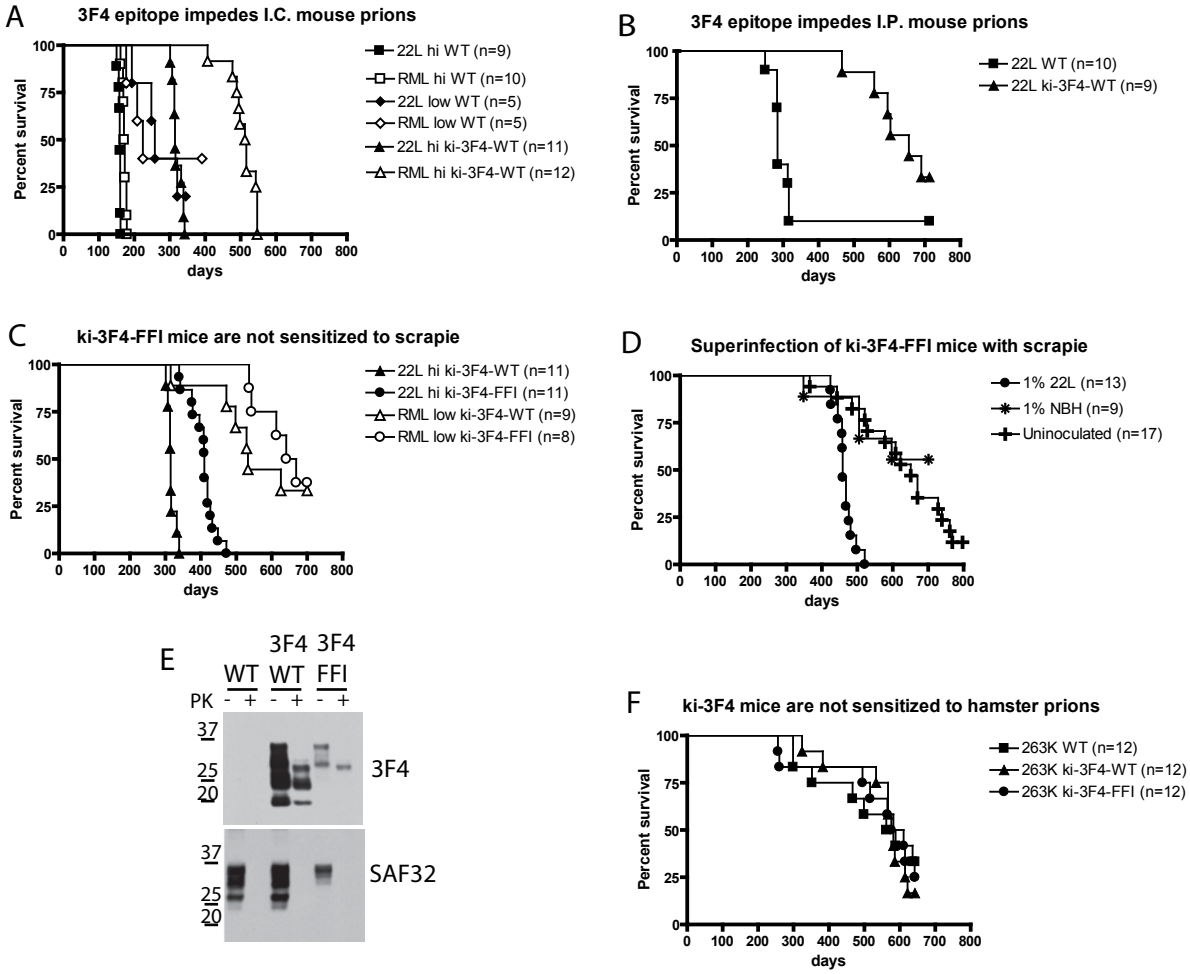

Supplemental Movies and Spreadsheets

Click here to download Supplemental Movies and Spreadsheets: Jackson movie S1.wmv

Supplemental Movies and Spreadsheets

Click here to download Supplemental Movies and Spreadsheets: Jackson movie S2.wmv

Supplemental Text and Figures

Supplemental Movie 1. Tga20 mice injected with ki-3F4-FFI brain homogenates. After a one year incubation period, Tga20 mice develop a highly unusual paroxysmal twitching of their hindlimbs, often immediately before or after scratching. They also develop kyphosis, pruritus, and an ataxic gate.

Supplemental Movie 2. Tga20 mice injected with brains from non-diseased mice (as well as Tga20 mice not injected at all, not shown) lack the clinical symptoms seen in the Tga20 mice injected with ki-3F4-FFI brain homogenates.

SUPPLEMENTAL DATA

SUPPLEMENTAL EXPERIMENTAL PROCEDURES

Generation of *Prnp* targeting constructs and ESCs.

Genomic plasmids VectorA, VectorC, and p129PrP were described in (Moore et al., 1995) and used as starting materials for our targeting constructs. We did not modify the knock-out clone (Vector C). To simplify the generation of several exchange constructs, we first added small linkers flanking the open reading frame (ORF) of Prnp. This was done by cloning a 2.2kb EcoRI fragment from the p129PrP into the EcoRI site of pBTIIKS(+), making pWJPrP31. An EagI restriction site was added downstream of the ORF by PCR site directed mutagenesis (PCRSDM) following the kit manufacturer's protocol (of pWJPrP31 using primers (5'-GTGGGATGAGGGCGGCCGTCCTGCTTGTTC-UPPER) (5'-GAACAAGCAGGACGGCCGCCCTCATCCCAC-LOWER) and a ClaI site was created by using primers (5'-GCCAAGGTTCGCCATCGATGACTGATCTGC-UPPER) (5'-GCAGATCAGTCATCGATGGCGAACCTTGGC-LOWER), inserting a guanine immediately before the translation start site yielding plasmid pWJPrP34. Vector A is an intermediate construct that has the extreme ends of the targeting homology but lacks the EcoRI fragment mentioned above. ClaI and EagI restriction sites in the backbone of Vector A were mutated by digestion with the corresponding restriction enzymes followed by blunting using mung bean nuclease for EagI or Klenow plus dNTP for ClaI, to make pWJPrP32. A 2.2kb EcoRI fragment was isolated from pWJPrP34 and ligated into the corresponding site of pWJPrP32, yielding pWJPrP38. A mouse PrP ORF containing methionine codons for positions 108 and 111 was cloned into pBTIIKS (+) in a manner

where the ClaI site is next to the 5' end of the PrP ORF, and EagI site is next to the 3' end of the ORF, yielding pWJPrP1. pWJPrP1 was then modified by PCRSDM to make the D177N mutation by using the following primers; (5'-CAGAACAACTTCGTGCACAATTGCGTCAATATCACCATC-UPPER) and (5'-GATGGTGATATTGACGCAATTGTGCACGAAGTTGTTCTG-LOWER) to make pWJPrP5. 0.8 kb EagI-ClaI fragments were isolated from pWJPrP1 and pWJPrP5 and ligated into the corresponding sites of pWJPrP38 to generate exchange targeting constructs pWJPrP41 and pWJPrP43, respectively. The result is the modification to the PrP ORF as well as the inclusion of the following linker sequences; GATAAGCTT between base -1 and +1 with respect to translation start site, and ATCCACTAGTTCTAGAAG at the third base pair position downstream of the translation termination sequence. These constructs were linearized by XhoI prior to electroporation. All enzymes purchased from New England Biolabs, Ipswich, MA. DNAs subjected to PCR or restriction digestion and ligation were sequenced.

A *Prnp* knock-out ESC line was generated by electroporation (300V, 250 μF) of $1x10^7$ HM-1 ESCs (Magin et al., 1992; Selfridge et al., 1992) in 1 mL of ESC media, using 50 μg of ClaI linearized vector C (Moore et al., 1995) and plated onto tissue culture plates pre-coated with gelatin and feeder cells. The next day, fresh media supplemented with HAT and Gancylovir selection agents was added. Selection was maintained for six days. Resistant colonies were tested by PCR and Southern analysis (described below). Properly targeted cells were then electroporated with exchange constructs in a two electroporation process. Cells were resuspended in cytomix (120 mM KCl; 0.15 mM $CaCl_2$; 10 mM K_2HPO_4/KH_2PO_4, pH 7.6; 25 mM Hepes, pH 7.6; 2 mM EGTA, pH 7.6; 5

mM $MgCl_2$; plus 2mM ATP, pH 7.6 and 5 mM glutathione added immediately prior to resuspension)(van den Hoff et al., 1992) at $1.25x10^7$ cells/mL. 0.8 mL of cells was added to a cuvette with 15 ug exchange construct. Cells were electroporated first with 400V at 950 μF, then at 400V at 500 μF, with 15 μg more exchange construct added between electroporations. Cells were plated as before, and split five days after electroporation into media containing 6-thioguanine. Resistant colonies were picked two weeks later and screened by PCR and Southern analysis for proper gene-targeting. The electroporator (GenePulser Xcell with the capacitance extender (CE) module) and 4 mm electroporation cuvettes were from Biorad, Hercules, CA.

Genotyping

PCR is performed using primers that flank the downstream insertion site with the following sequences (5'-GAGCAGATGTGCGTCACCCAG-upper) and (5'-GAGCTACAGGTGGATAACCCC-lower). PCR products from unmodified alleles are 207 bp and those from knock-in alleles are 225 bp, easily resolved with 3% agarose gels. The third band produced in PCR with heterozygous cells or animals is due to impaired migration of heteroduplex DNA. These heteroduplexes can also be formed by mixing PCR products from homozygous WT and knock-in mice, melting the DNA and allowing it to renature, indicating there is not an unexpected chromosome rearrangement in heterozygous animals.

PCR positive ESC clones were further tested by Southern blotting using conventional methods (Sambrook et al., 1989). A 3' probe was isolated from p129PrP using EcorV and BamHI. This probe shares no homology with the exchange or knock-out vectors and

therefore only detects chromosomal ESC DNA. Genomic DNA was digested with BamHI, to detect a new restriction site in the modified allele. These 129/Ola (Ola) derived ESCs were then injected into C57Bl/6Taconic (B6) 3.5 day old blastocysts to generate chimeric animals. Chimeras were bred to B6 mice to generate F1 animals. F1 animals were bred to B6 mice to generate F2 animals. F2 heterozygous animals were intercrossed to generate mice that were homozygous knock-in or homozygous WT. Homozygous mice were then bred to produce large enough litters for experiments. During the crossing with B6 mice, in addition to tracing PrP alleles, we followed the inheritance of the wild-type *Hprt* allele using a PCR assay (McEwan and Melton, 2003) in order to eliminate the *Hprt* deletion from the HM-1 cells from our colony.

Husbandry

The animal facility is designated as specific pathogen free, with a series of barriers, including restricted access, multiple doorways, isolation cubicles, and filter-topped mouse cages. Sentinel mice are tested regularly for pathogens. Technicians check cages daily with respect to water, food (provided *ad libitum*), and cleanliness as well as the general health of the animals. Cages are changed twice weekly. Technicians do not interact with animals during video recording. Three different rooms are used to separate 1) scrapie infected mice from 2) the general population of mice and mice in 3) behavioral experiments and mice involved in *de novo* FFI prion transmission experiments. Mice in room 3 are divided into separate cubicles.

Supplemental Tables

Supplementary table 1 Transmission of ki-3F4-FFI disease

innoculum	Ki-3F4-WTvs.:	P value[a]	Tga20 vs.:	P value[a]
Primary-#1	WT	.0065	WT	.014
	KO	.0027	KO	.0067
Primary-#2	WT	.0175	WT	.0027
	KO	.0015	KO	.0027
Primary-#3	WT	.0001	WT	.0002
	KO	.0029	KO	.0060
Secondary-#1	KO	.0001		
Secondary-#2	KO	.0132		

[a] P value calculated by Log-rank test

Supplementary table 2 Scrapie transmission

Corresponding figure	Comparison	P value [a]
5a	22L hi WT vs. 22L hi ki-3F4-WT	<.0001
5a	RML hi WT vs. RML hi ki-3F4-WT	<.0001
5a	22L low WT vs. 22L hi ki-3F4-WT	<.05
5a	RML low WT vs. RML hi ki-3F4-WT	<.005
5b	22L WT vs. 22L ki-3F4-WT	<.005
5c	22L hi ki-3F4-WT vs. 22L hi ki-3F4-FFI	<.0001
5c	RML low ki-3F4-WT vs. RML low ki-3F4-FFI	>.1
5d	1% 22L vs. 1% NBH	<.0005
5d	1% 22L vs. uninoculated	<.0001
5d	1% NBH vs. uninoculated	>.1
5f	263K WT vs. 263K ki-3F4-WT	>.5
5f	263K WT vs. 263K ki-3F4-FFI	>.5
5f	263K ki-3F4-WT vs. 263K ki-3F4-FFI	>.5

[a] P value calculated by Log-rank test

Supplemental Figure Legends

Figure S1. Two step gene-replacement approach to generate knock-in ES cells and mice. Horizontal lines with labeled boxes superimposed on them represent double stranded DNA. The boxes correspond with exon 3 of the mouse Prnp gene. The box labels indicate the protein coding sequence for that DNA sequence. Long horizontal lines with diagonal breaks near the ends represent genomic DNA. The diagonal breaks represent conceptual breaks in the continuity of the genomic DNA to indicate the genomic DNA represented in the schematic is only a tiny portion of the entire chromosome. Short horizontal lines represent recombinant DNA plasmids used to manipulate genomic DNA. The two step "tag and exchange" method of gene-targeting was used to replace the entire protein coding sequence of Prnp with DNA sequence encoding mutated PrP open reading frames in mouse embryonic stem cells (ES cells). For the first step, a "tag construct" undergoes homologous recombination (depicted by large "X" like crosses) with one endogenous *Prnp* allele (labeled "endo"), resulting in deletion of a section of *Prnp* and insertion of a hypoxanthine phosporibosyltransferase (*Hprt*) minigene, resulting in a knock-out allele (KO). The presence of the *Hprt* minigene confers resistance to HAT media which will kill ES cells lacking the *Hprt* minigene. For the second step, KO ESCs were then modified with an exchange construct which replaces the Hprt minigene with the mutated PrP open reading frame sequence via homologous recombination. The "knock-in PrP" allele differs from the wild-type Prnp allele by the inclusion of a BamHI restriction endonuclease site (B) adjacent to the open reading frame ("3F4-PrP" boxed), which can be detected by genomic Southern analysis using a probe (P) which is homologous to a region of Prnp downstream of the targeting constructs. Correctly

targeted ESCs were injected into C57Bl/6 Taconic embryos 3.5 days post fertilization. Injected embryos were then implanted into pseudopregnant females (CD1). Resulting chimeric mice derived from host embryo and donor ES cells were then bred to C57Bl/6 mice to establish the knock-in mouse lines.

Figure S2. Additional examples of MEMRI scans of knock-in mice.
Top, MEMRI scan of another ki-3F4-WT mouse. Lower, MEMRI scans of 3 more ki-3F4-FFI mice. Mice with prominent clinical signs (ataxia, reduced body condition, or kyphosis) showed the most prominent MEMRI abnormalities.

Figure S3. Heavily vacuolated deep cerebellar white matter in ki-3F4-FFI mice.
Aged but otherwise normal ki-3F4-WT cerebellum (left) has very few vacuoles. H&E stained paraffin sections show vacuolation in a ki-3F4-FFI mouse (right).

Figure S4. Severe loss of thalamic neurons.
Nissl stained stained 30 μm thick sagittal sections, from ki-3F4-WT (left), and from ki-3F4-FFI mice (right). Note the ki-3F4-FFI sections have fewer neurons (large white spots) yet more non-neuronal cells (small white spots), most of which are likely glial cells. Dark areas in top right of each panel are ventricles. Distance from midline is indicated to the left of each row.

Figure S5. Phenotypic arrays of AMBA data.

(A) Tile panels showing the fold difference (left) and P-values (right) from comparisons ki-3F4-WT and WT mice. This comparison was performed to gage the amount of noise intrinsic to this technique. The colored P-values tiles are scarce and randomly distributed.

(B) A pair of tile panels showing the fold difference (left) and P-values (right) from comparisons of ki-3F4-WT and ki-3F4-FFI mice. For all panels, yellow tiles represent behaviors performed more by the indicator line (WT or ki-3F4-FFI mice) than the standard line (ki-3F4-WT mice), and blue tiles represent behaviors performed less by the indicator lines. The age in months is indicated immediately below each panel, the number of mice used in each comparison is immediately above each panel. Behaviors reported in this figure show all possible behaviors analyzed (although "urinate" was not analyzed and "circle" is prone to error). A similar panel is displayed in Fig. 3 of the main manuscript, differing in that behaviors there were combined to allow for a simpler array (details in methods section). P-values are calculated using a non-parametric (Wicoxon rank-sum) test to buffer against effects of highly uncharacteristic scores which are inevitable in this type of non-task dependent behavioral assay. The following behaviors were condensed to give the corresponding behavior names in Fig. 3b: pause and stationary condensed to still; rear up to partially reared, remain partially reared, and come down to partially reared were condensed to half reared; rear up from partially reared, rear up, and remain rear up were condensed into fully reared; come down from partially reared and come down were condensed to return to floor; hang vertically from rear up, remain hang vertically, and hang vertically from hang cuddled were condensed to vertical hang; hang cuddled and remain hang cuddled were condensed to cuddled hang; walk

slowly, walk left, and walk right were condensed to travel; unknown behavior and no data were condensed to unassigned. Hang vertically and urinate are not analyzed and circle scoring is unreliable.

Figure S6. Fluctuation in Tb of ki-3F4-FFI mice.

(A) Tb of an individual ki-3F4-WT mouse (WT 2, red) overlayed on a line representing the average Tb of 5 ki-3F4-WT mice (WT avg, black), top left. Tb of 3 ki-3F4-FFI mice (FFI 3, 4 , 5, blue lines top right and both bottom panels) plotted over the same WT avg line (black) as the top left panel and the 3 "c" panels in Fig. 3 of the main manuscript. Temperatures are recorded every 5 minutes, 288 measurements per day.

(B) Bar charts of the above mentioned data showing the average number of epochs during which the temperature change was less than 0.1°C (left), or greater than 1°C (right). Epoch lengths considered are labeled below the charts. Error bars indicate standard error of the mean. P-values calculated by Student's two-tailed T test. One star indicates $P< 0.05$, two stars indicate $P< 0.01$.

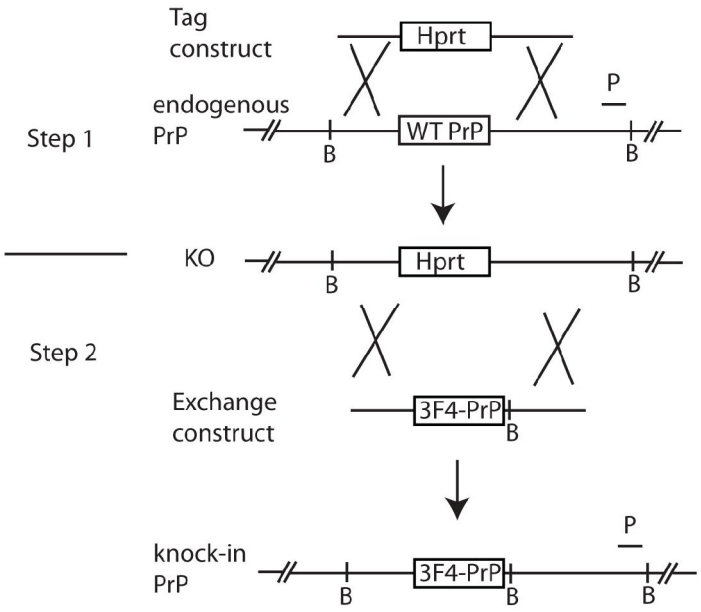

Supplemental Figure 1

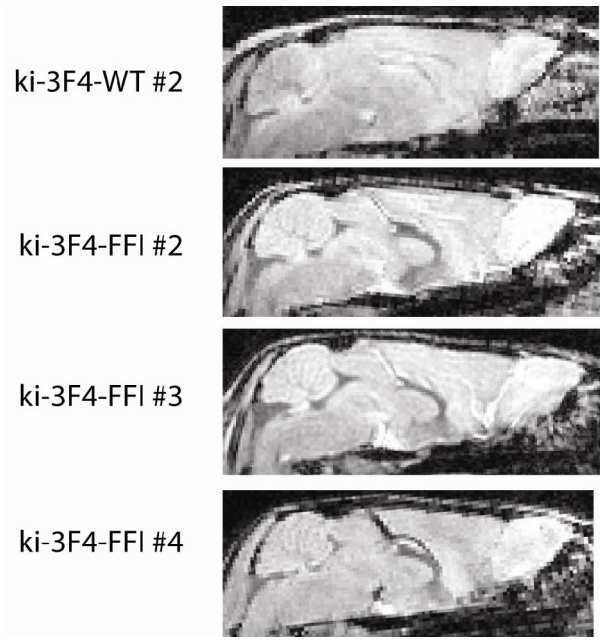

Supplemental Figure 2

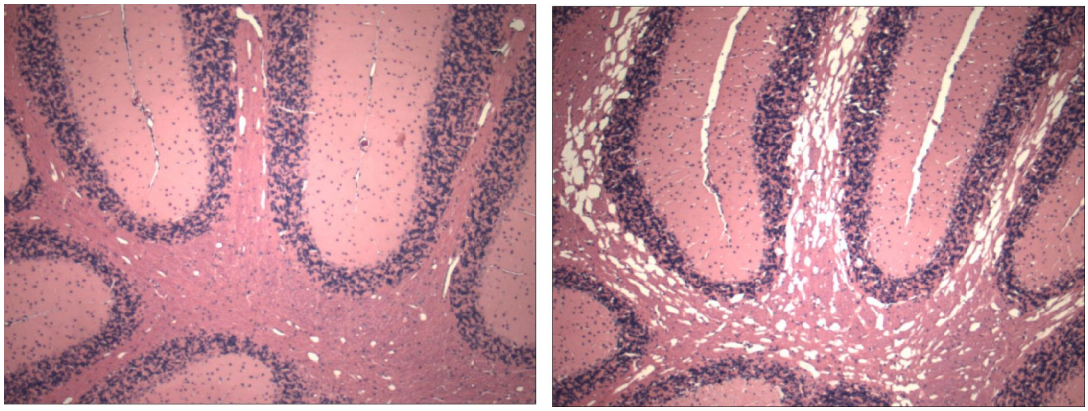

Supplemental Figure 3

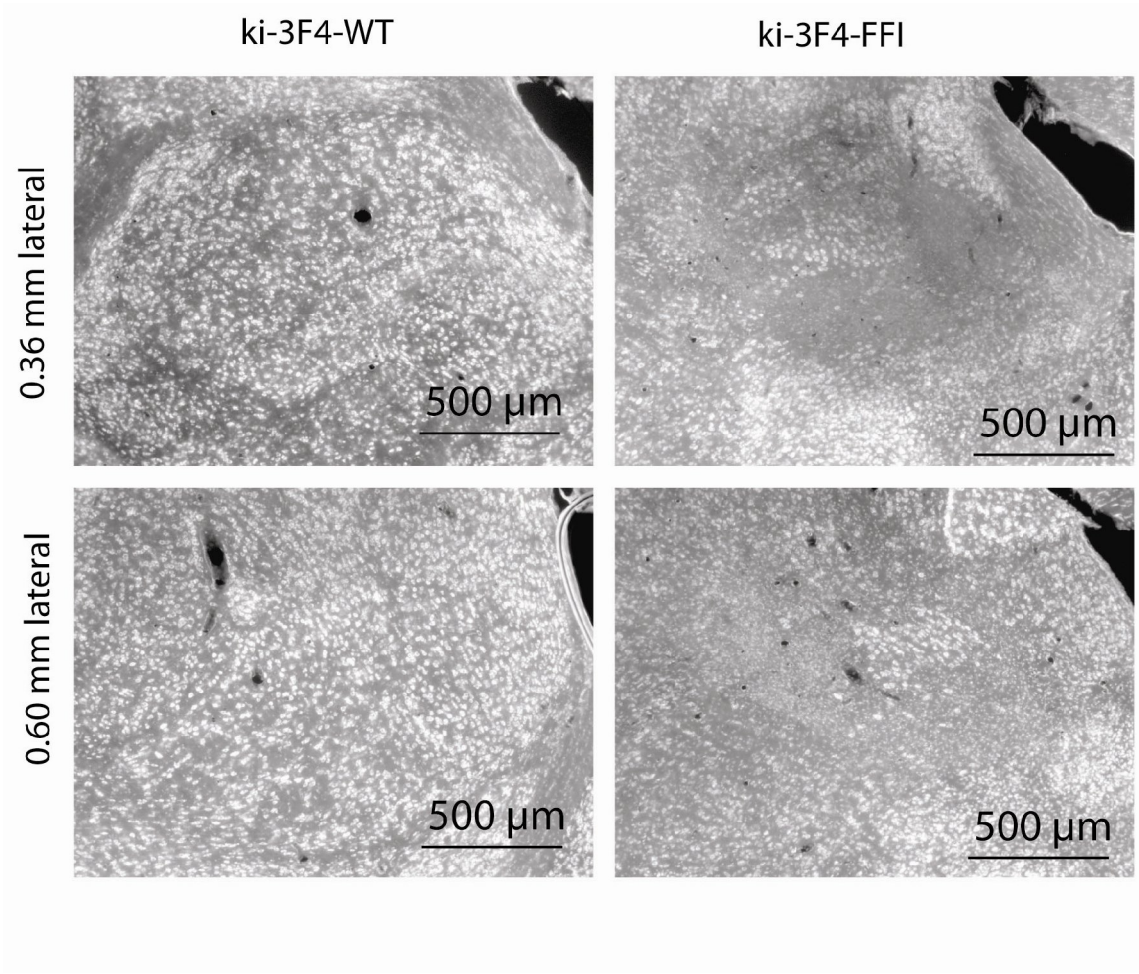

Supplemental Figure 4

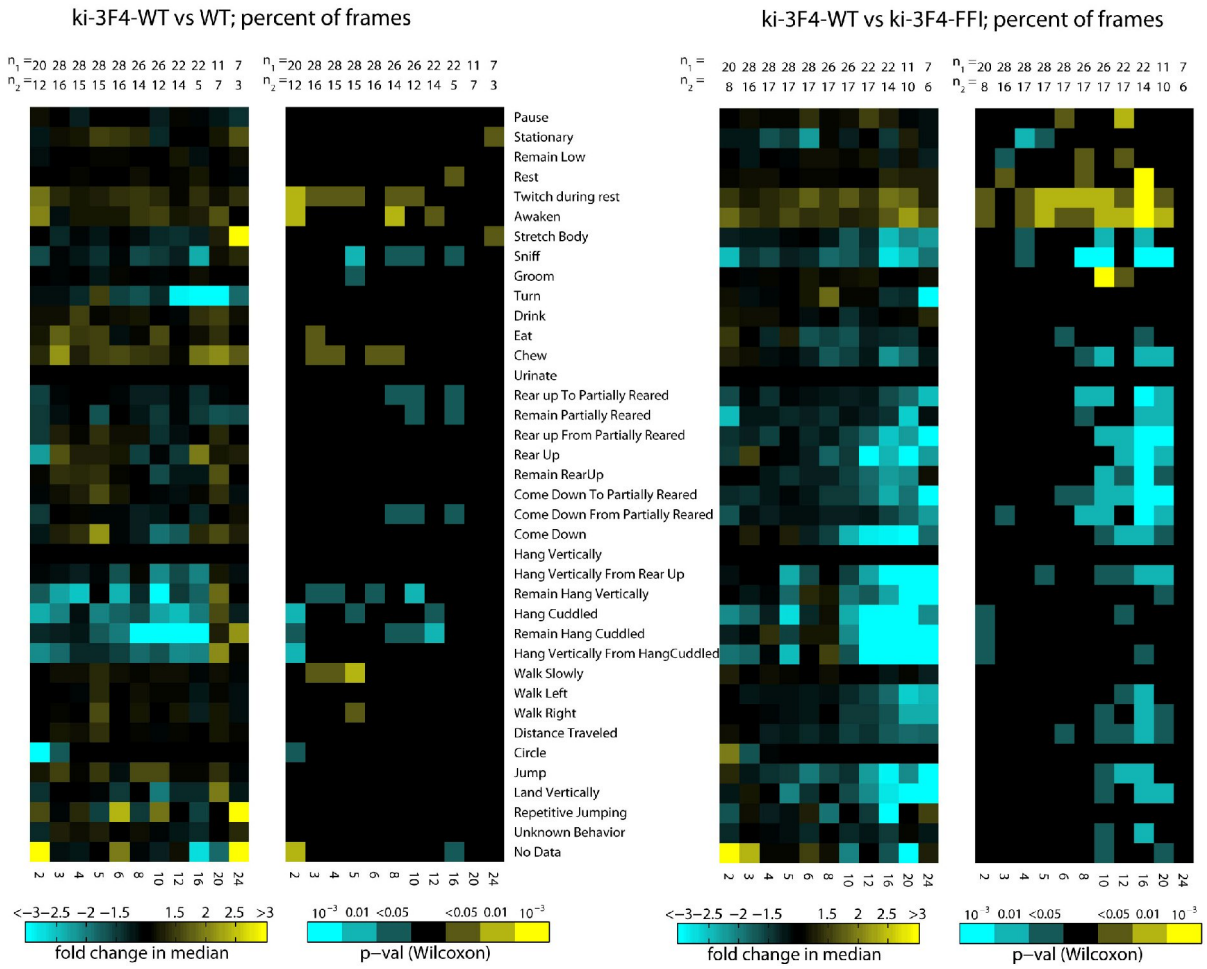

Supplemental Figure 5

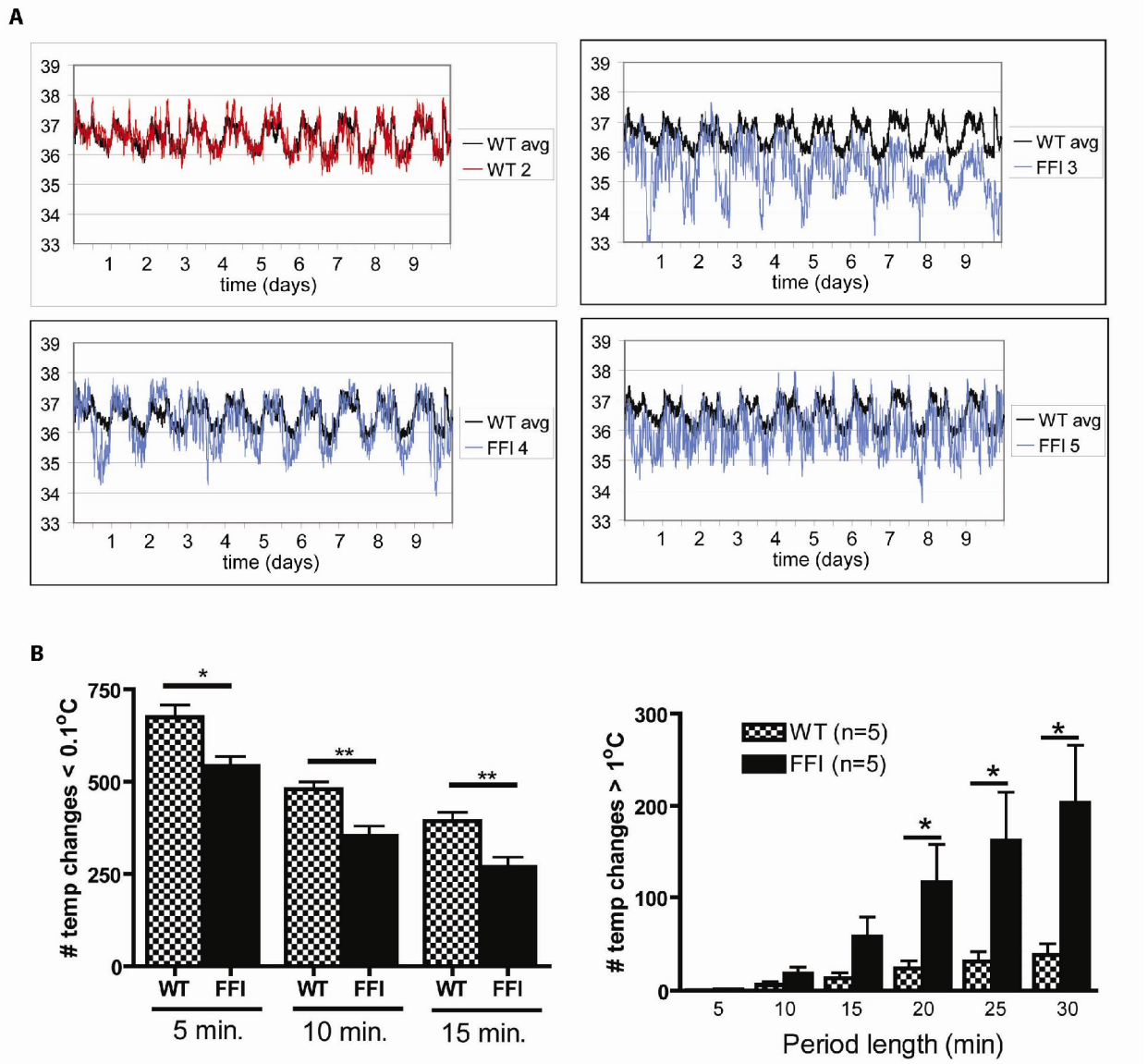

Supplemental Figure 6

Supplemental References

Magin, T.M., McWhir, J., and Melton, D.W. (1992). A new mouse embryonic stem cell line with good germ line contribution and gene targeting frequency. Nucleic Acids Res *20*, 3795-3796.

McEwan, C., and Melton, D.W. (2003). A simple genotyping assay for the Hprt null allele in mice produced from the HM-1 and E14TG2a mouse embryonic stem cell lines. Transgenic Res *12*, 519-520.

Moore, R.C., Redhead, N.J., Selfridge, J., Hope, J., Manson, J.C., and Melton, D.W. (1995). Double replacement gene targeting for the production of a series of mouse strains with different prion protein gene alterations. Biotechnology (N Y) *13*, 999-1004.

Sambrook, J., Fritsch, E.F., and Maniatis, T. (1989). Molecular cloning : a laboratory manual, 2nd edn (Cold Spring Harbor, N.Y.: Cold Spring Harbor Laboratory).

Selfridge, J., Pow, A.M., McWhir, J., Magin, T.M., and Melton, D.W. (1992). Gene targeting using a mouse HPRT minigene/HPRT-deficient embryonic stem cell system: inactivation of the mouse ERCC-1 gene. Somat Cell Mol Genet *18*, 325-336.

van den Hoff, M.J., Moorman, A.F., and Lamers, W.H. (1992). Electroporation in 'intracellular' buffer increases cell survival. Nucleic Acids Res *20*, 2902.